

December 14, 2015

Dr Jatin Kala
Topical Editor
Geoscientific Model Development Discussions

Dear Dr Kala.

Re: The GEWEX LandFlux project: evaluation of model evaporation using tower-based and globally-gridded forcing data by McCabe et al. (2015).

We appreciate your solicitation of the three independent reviewers for our recently submitted journal article (reference GMD-2015-142). As you will see in the attached author response, we have responded comprehensively to each of (what we consider) the relatively minor comments from the reviewers.

All of the reviewers recognise the importance of this work, which is satisfying given the time and effort that has been expended in developing these global flux products over the last several years. I would reiterate that this is the first and only such global exercise to evaluate multiple flux models over such an extended period of time and across multiple biome and climate types in such a consistent manner. Given that this will be the principal reference for the GEWEX Landflux data product, we anticipate a considerable interest in the research.

If there are any further queries that you or your editorial staff may have in regard to this manuscript, please do not hesitate to contact me at your convenience.

Best wishes,

A handwritten signature in black ink, appearing to read 'Matthew McCabe', is centered below the text 'Best wishes,'.

Matthew McCabe

Professor of Hydrology and Land Observation
King Abdullah University of Science and Technology

Response to Joshua Fisher (RC C2089)

Author Response. We appreciate the insightful comments by Dr Fisher, particularly in regard to elaborating the context of the GEWEX Landflux study and its differentiation from prior analysis. We have attempted to address these points in the responses below.

Reviewer Introduction. This is a well-written study intercomparing 4 ET algorithms against FLUXNET ET measurements. Like the rest of the group of papers coming out of this team (GEWEX/LandFlux, WACMOS), the strengths are in the selection of algorithms, the common forcings, and the rigorous analyses. Similarly, the weaknesses include the fact that the results are scattered among different papers with somewhat different details of analyses, so it is very difficult to understand the cohesive picture, and that the papers do little to go beyond statistical intercomparison and into the realm of science understanding.

Comment 1. Nomenclature consistency: Mu et al., 2011 abbreviation is referred to inconsistently across projects, i.e., PM-Mu, PM-MOD, PM-MOD16, etc. Same goes with GLEAM (colon/no-colon; Methodology vs. Model).

Author Response. *The reviewer raises an important point. It is worth noting that there are a number of versions of the Mu et al. 2011 that have been published in the literature over the last few years. Here we employ the most recent iteration, which has also appeared in a number of earlier papers from our group (where it is referred to as PM-Mu). In order to be consistent with these previous efforts (and past work including the Vinukollu et al. papers), we have retained the current usage. We now make a note in Section 2.2.3 that although the abbreviations are distinct, the models are consistent across both the Landflux and WACMOS-ET projects. We defer to the Miralles et al. (2015) paper and adjust the use of GLEAM to be consistent with that contribution.*

Author Change. *The following note is included at the start of Section 2.2.3 to highlight the commonality of models across projects, even though the abbreviation is different: “(n.b. the PM-Mu nomenclature used herein reflects an identical model used in Michel et al. (2015) and Miralles et al. (2015), where it is referred to as PM-MOD)”.*

Reference to GLEAM follows Miralles et al. (2015) as the Global Land Evaporation Amsterdam Model and has been adjusted where relevant throughout the manuscript.

Comment 2. It should be made clear how this study advances past Vinukollu et al 2011.

Author Response. *The Vinukollu et al. (2011) paper presented an excellent multi-model evaluation of global flux products. However, there are some key differences and advances between this and our current contribution. Firstly, the scale and scope of the analysis: in their paper, Vinukollu studied the period 2003-2006 and compared global scale simulations against 12 flux towers in the US. We examine data from 45 globally distributed (three-quarters outside of the US) and consistent towers (i.e. all towers are used across all models), spanning a period of approximately 10 years (with an average tower record length of more than 4 years). Most importantly, in the Vinukollu study, no analysis of the models was performed at the tower-scale: a key feature of the present work. That is, in examining model response, both large-scale gridded*

forcing and small scale tower forcing are employed. Additionally, Vinukollu et al. present their analysis at a monthly and annual scale, whereas we examine the finest time resolution of 3-hourly: the first such attempt to do so. Finally, the emphasis in the Vinukollu paper was on developing a satellite driven forcing dataset, whereas we have attempted to assemble a high-quality and consistent forcing product at the grid-scale, irrespective of a remote sensing focus.

Vinukollu RK, Wood EF, Ferguson C and Fisher JB (2011) "Global estimates of evapotranspiration for climate studies using multi-sensor remote sensing data: evaluation of three process-based approaches", Remote Sensing of Environment, 115, 801-823

Comment 3. Also, please make clear how this is *scientifically* different than the Michel paper (in prep at the time of this review writing, but soon to be in Discussions). At first, when reading the Michel paper, I thought the main difference was the 3-hourly analysis, but then I've seen the McCabe paper also includes 3-hourly...

Author Response. *It is important to highlight that WACMOS-ET is a direct contribution to the GEWEX Landflux efforts, and by no means are these projects competing efforts. As a consequence, there is involvement by key investigators driving these efforts in both projects and deliberate commonalities between the projects. But there are also clear distinctions. The most obvious of these is the motivation behind them. Landflux is focused on the development of long-term (20+ year), climate scale data records, while WACMOS-ET examines a short-term (2005-2007) period focused on demonstrating evaporation capability using predominantly European Earth-observing assets. As such, there are clear distinctions in the forcing data used to drive the models. Apart from the more compressed period of analysis in the WACMOS-ET study, the compilation of distinct elements in the forcing data-set allows for an examination of model response to different forcings: work that remains ongoing to tease out these influences. Encouragingly, the outcomes of these two projects seem largely consistent in terms of simulation behavior, even though the assessment period was considerably longer in the McCabe et al. analysis [and also used a greater number of towers: 45 versus 24]. Michel et al. expand the Landflux focus on 3-hourly analysis to the daily scale, while also investigating variation during night and day conditions. Both projects represent significant contributions towards the goal of developing robust global flux products.*

Author Changes. *Now that the WACMOS-ET papers are in HESS Discussion, we make explicit reference to these works when discussing the different scientific rationales behind the efforts in the Introduction.*

*Michel D, Jiménez C, Miralles DG, Jung M, Hirschi M, Ershadi A, Martens B, McCabe MF, Fisher JB, Mu Q, Seneviratne SI, Wood EF and Fernández-Prieto D (2015). "The WACMOS-ET project – Part 1: Tower-scale evaluation of four remote sensing-based evapotranspiration algorithms." Hydrol. Earth Syst. Sci. Discuss. **12**(10): 10739-10787.*

*Miralles, DG, Jiménez C, Jung M, Michel D, Ershadi A, McCabe MF, Hirschi M, Martens B, Dolman AJ, Fisher JB, Mu Q, Seneviratne SI, Wood EF and Fernández-Prieto D (2015). "The WACMOS-ET project – Part 2: Evaluation of global terrestrial evaporation data sets." Hydrol. Earth Syst. Sci. Discuss. **12**(10): 10651-10700.*

Comment 4. Speaking of which, given the whirlwind of papers coming out of this GEWEX/LandFlux & WACMOS group (e.g., Michel, Miralles, McCabe, Ershadi,...), I strongly urge McCabe in particular to write a meta-analysis/review paper of these papers to distill everything down into 1 place (include the Vinukollu, Jimenez, Mueller, etc. papers too). Aim high (e.g., one of the Natures, etc., or perhaps WRR).

Author Response. *This is an excellent suggestion that is indeed on the radar of the respective investigators of these efforts. A distillation of past work, progress and the way forward would be a valuable contribution to the literature. We hope to rely on other participants in the evaporation community to assist with this effort!*

Comment 5. A semantic nuance that would improve the interpretation of the results further would be to rephrase/reframe model performance not so much in that X model overestimates/underestimates, but that it's actually the model in conjunction with the selected forcings. E.g., it may not be inherent to the model itself that it is biased high or low, but rather due to the forcings. This would primarily be for bias, not as much for the other statistics, though the other statistics would not necessarily be completely immune either.

Author Response. *We agree with the reviewer that discriminating the role of model response separate to uncertainties in forcing is a needed task. We have attempted to restate that it is the combined influence of forcing and model response that is being examined - and to which further work is required to disentangle. Indeed, the title of Section 3.1 highlights that we are undertaking a "relative performance" of the models when comparing tower and gridded data. The paragraph at the bottom of page 6826 further reinforces this concern:*

"Overall, these results confirm that all models display a relatively high sensitivity to changes in the type and quality of input forcing data. While gridded forcing data are expected to have a mismatch with the tower-based forcing due to their larger pixel (and footprint) sizes, this spatial mismatch will impact all of the applied models, albeit to a lesser or greater extent, depending on forcing data requirements. While spatial scale no doubt plays a major role in decreasing model efficiencies at grid-scales, the most likely reason for the differences in tower- versus grid-based results relates to internal inconsistencies within the gridded forcing data....Not surprisingly, results also indicate that those models that use fewer inputs show lower sensitivity to changes in the forcing. As such, any inconsistency between the tower and gridded data is likely to have less influence on the PT-JPL, GLEAM and PM-Mu models than it will on SEBS, which in addition to vegetation height, requires both land surface temperature and wind speed data: two variables with considerable spatial variability"

The Landflux focus is to develop (as much as possible) consistent forcing across models, presenting one means to address this complicated task. But we also need to recognise that forcing uncertainties are unavoidable and will always influence simulation results. Characterizing this response requires further attention.

Author Changes. *We have added the following sentence to the above paragraph to reflect the combined nature of model and data uncertainty: "Disentangling the varying influence of model*

structural and forcing data uncertainty requires focused attention and is examined further in the Discussion section”.

Comment 6. How can error be reduced in the models further? What causes the error? I think a lot of the error that the authors attribute, as calculated, to the models is in fact error in the data. It remains an outstanding question in this analysis why a model would do well at some sites, but not well at other very similar sites. Or, even inconsistently throughout time within a single site.

Author Response. *The Landflux and WACMOS-ET efforts are initial attempts at addressing these types of questions (with the realization that undertaking such works seem to uncover more questions than answers). The challenge of separating the role of process descriptions, model sensitivity to forcing and forcing data uncertainty is an outstanding one that requires sustained community effort to resolve. These questions of attribution are critically important and require continued examination. However, they cannot be done in isolation. Studies such as the present analysis illustrate the inherent variability in performance and multi-model response and provide solid first steps towards addressing such questions. In the related WACMOS-ET contribution, Miralles et al. (2015) offer some initial guidance on model behaviour that developers may be able to address. For instance, the underestimation in PM-Mu/MOD is due to an overestimation of evaporative stress, that PT-JPL and GLEAM underestimate in high-latitudes and times of low radiation, and that the role of interception (and partitioning of evaporation between its different components) remains a major source of uncertainty.*

Miralles et al. (2015) “The WACMOS-ET project – Part 2: Evaluation of global terrestrial evaporation data sets”, Hydrol. Earth Syst. Sci. Discuss., 12, 10651–10700, doi:10.5194/hessd-12-10651-2015

Response to Anonymous Reviewer #3 (RC C2847)

Author Response. We thank the anonymous reviewer for their thoughtful comments on our manuscript. Following is a point-by-point response to the issues and suggestions raised.

Comment 1. Address footprint of tower flux observations and how those model is capable to explicitly treat sub-grid variability. If not, the evaluation cannot guarantee the comparisons are not biased. Screening out tower flux measurements over heterogeneous footprint also helps.

Author Response. *The issue of footprint analysis is certainly of interest in high-resolution flux retrievals, especially where spatial variations can be resolved at the pixel scale. However, in our analysis, the gridded data completely covers any within-footprint scale impacts: by at least one order of magnitude. Tower data are influenced by the tower-footprint (which in addition changes per sensor, thus per measured variable), but this is an inherent element of flux-tower analysis. Sub-grid scale variability is not explored here, since it is well beyond the scope of the analysis. Regardless, none of the models explicitly account for this, beyond those that include fractional cover measurements (which likely represent most subgrid variability). Point-scale tower meteorological forcing is assumed to be areally representative (as there is no other alternative). One of the unique aspects of this work is that tower data are consistent across all model simulations: that is, tower-bias is minimized, by ensuring that all models are assessed against the same tower records. Further, the tower-to-grid scale analysis also acts as a diagnostic of representativeness and point-to-pixel error (apart from forcing uncertainty). Screening out “heterogeneous” landscapes (most are heterogeneous even at the tower scale) would unreasonably restrict any evaluation of flux retrievals from ever being undertaken: including those performed here. Here we accept the inevitability of real-world heterogeneity and include this as an inherent element of our intercomparison study.*

Author Changes. *Table A1 has been updated to include tower height, in addition to ground elevation, as an indirect measure of the tower fetch. We also highlight the inevitable nature of heterogeneity in the landscape in the Introduction through the following sentence: “One of the unique aspects of the present study is that tower data are consistent across all model simulations: that is, tower-bias is minimized, by ensuring that all models are assessed against the same tower records. Further, even though sub-grid scale variability is not explored here (since none of the models explicitly account for this), the tower-to-grid scale analysis acts as a diagnostic of representativeness and point-to-pixel error.”*

Comment 2. How climate zones are determined? Since those models are mainly based on energy and water balance and availability, physical criteria should be explicitly provided. In that sense, additional analysis or replacement for 3.3 over Budyko climate regime and the curve.

Author Response. *Climate zones are specified in the metadata of each of the Fluxnet tower locations, which are ultimately derived from Rubel and Kottek (2010) “[Observed and projected climate shifts 1901-2100 depicted by world maps of the Köppen-Geiger climate classification](#)”, Meteorol. Z., **19**, 135-141. DOI: [10.1127/0941-2948/2010/0430](#). This is the standard approach to climate classification, so has been retained for this analysis. A statement describing the classification has been included in Section 2.1.4.*

Author Changes. *The following statement is included in Section 2.1.4: “These zones were prescribed from the tower-specific metadata, which were in turn derived from Rubel and Kottek (2010) based on a Köppen-Geiger climate classification”.*

Comment 3. Provide additional information for evaluation of grid-based forcing data quality. Knowing the character of error (i.e., phase mismatch or persistent offset) would be also very important.

Author Response. *The emphasis here has been placed on examining the variability in model response, rather than on variability in model forcing: principally because characterizing the impact of forcing uncertainty on the models themselves is a complicated (and under-studied) task. Within the context of this study, attributing model error to forcing error requires that the “true” forcings be known, which of course isn’t the case. Nonetheless, the reviewer correctly identifies an area of much needed further study.*

The focus of our analysis is to examine model performance in response to an operational forcing set, using tower data as a benchmark. Given that the analysis encompasses record lengths of (on average) 4 years (see Figure A1) and that the 15 or 30 minute tower data was upscaled to 3 hourly, a focused assessment on the forcing data is impractical. Importantly, any potential lag or phase mismatch would likely be removed in the temporal upscaling. Figure 7 and Figure 10 provide both R^2 and Nash-Sutcliffe efficiency metrics of comparisons between the 3 hourly gridded data and the temporally equivalent local-scale forcing across all of the 45 tower sites, for both climate zone and biome type. As can be seen, the correlation is very strong for all variables except for wind-speed (which is certainly one of the most challenging variable to match between scales).

The individual gridded forcing data products have been used previously in a range of analyses. As noted above, the purpose of our investigation is not to assess the quality of the forcing, but to examine the impact of these widely available datasets on the estimation of model derived evaporation. The issue of forcing quality and the impacts of this on product accuracy are regularly highlighted throughout the manuscript (see e.g. Abstract Line 5, Section 3.1 and elsewhere) and form key elements of the presented results. As highlighted in Section 3.1 (from Line 20), while we acknowledge that spatial scale plays a role, the impact of internal inconsistencies within the gridded data (i.e. the fact that data sets are derived from different sources) drive the inter-product differences.

Comment 4. If possible, aligning the analysis in previous researches with different types for models (e.g., land surface models and hydrologic models) will introduce additional values.

Author Response. *We are unclear what the reviewer is recommending here. In response to a query by Reviewer 2, we have provided some additional details on the differentiation of this work to previous analysis. This provides a clearer rationale for the current effort and places it in the context of prior work. An additional recommendation of Reviewer 2 was to provide a synthesis study that overviews the considerable research efforts that have driven global flux studies over the last few years: this will form the focus of future efforts. In terms of*

benchmarking the performance of evaporation models against GCM, LSM or reanalysis type output, we refer to the earlier and thematically related studies by Jimenez et al (2011) and Mueller et al. (2011, 2013).

*Jiménez et al. (2011). "Global intercomparison of 12 land surface heat flux estimates." J. Geophys. Res. **116**(D2): D02102*

*Mueller et al. (2011). "Evaluation of global observations-based evapotranspiration datasets and IPCC AR4 simulations." Geophysical Research Letters **38**(6)*

*Mueller et al. (2013). "Benchmark products for land evapotranspiration: LandFlux-EVAL multi-data set synthesis." Hydrology and Earth System Sciences **17**(10): 3707-3720.*

Comment 5. Additionally, this manuscript can be more concise. Remove or rephrase of speculations without any robust evidence (e.g., some sentences including ‘may’ or ‘perhaps’) would help.

Author Response. *We have attempted to avoid pure speculations. However, there remains much additional work that needs to be done to untangle some of the numerous issues related to global flux development. Speculation is an inevitable by-product of this. Where questions on the intangibles of our analysis remain, the intent is to highlight these issues and to assist in spurring on future research efforts. We have rephrased such terms as mentioned by the reviewer (“perhaps” now appears only once).*

Author Changes. *We have removed the line “likely due to variability in performance as a response to the land surface type or climate condition” on Page 6825, Line 24. We have replaced “perhaps” with “represents one of” in the Discussion on Page 6838, Line 23. “Perhaps” has been removed on Page 6838, Line 27.*

Response to Anonymous Reviewer #1 (RC C1874)

Author Response. We thank the anonymous reviewer for their thoughtful comments on our paper. In responding to these, we have itemized the various comments in order of their appearance in the response letter.

Comment 1. While I tend to agree this is an interesting and important study as we continue on the way of better global ET mapping, it has several issues. First of all, I do not think it is appropriate to compare ET estimates at the grid-cell scale (i.e., 0.5 in this case, or ~ 55 by 55 km) with flux-tower measurements (usually have a footprint of 1~2 km). The spatial heterogeneity in soil, vegetation and micro-climate can lead to large spatial variation in ET within one grid-box. This issue can be more strongly manifested if there were large variation in topography (leads to strong climate gradients) or vegetation type (the grid-box sits on the boundary of two biome types). Therefore, their conclusion regarding grid-box evaluation is no longer stand.

Author Response. *The reviewer raises an important point regarding the issue of scale in the evaluation of global flux products. Indeed, this largely reflects one of the motivations for undertaking this work: how to evaluate large-scale flux retrievals in the face of limited observations. The overriding rationale of this paper is **not** to use tower-based fluxes to “validate” grid-scale model simulations, but rather to understand how grid-scale fluxes compare with a parallel simulation exercise run at the tower of the scale. As noted in the Introduction (see line 29), “Understanding how application of gridded forcing data might influence the performance of the different models, relative to their performance when forced with (presumably) higher-quality tower data, is a motivating rationale for this work”. The models are deliberately run with both sets of forcing to examine the impact of scaling issues on flux response: a very standard approach to assess such behavior. Indeed, this provides an indirect assessment of the footprint mismatch, which is explicitly recognized in Paragraph 2 of Section 3.1, as well as in Figures 7 and 10, which highlight the strong correlation between variables at these opposing scales.*

In the absence of any alternative means of assessment, making use of an extensive record of tower-based fluxes is certainly an appropriate method by which the behavior of large-scale fluxes can be examined. Determining alternative metrics of performance (i.e. the hydrological consistency approach of McCabe et al. 2008) is an area of ongoing investigation.

McCabe MF, EF Wood, R Wójcik, M Pan, J Sheffield, H Su and H Gao (2008) “Hydrological consistency using multi-sensor remote sensing data for water and energy cycle studies” Remote Sensing of Environment, 112(2): 430-444

Comment 2. In this sense, secondly, a big concern is what is the advancement of this study over a recently published paper in AFM (also conducted by the same group of authors, i.e., Ershadi et al., 2014, Multi-site evaluation of terrestrial evaporation models using FLUXNET data, AFM). In Ershadi et al. (2014), four models (three of them are used in this study, including PT-LPJ, SEBS, and PM-Mu) were evaluated at 20 flux sites, most of which (or all, I did not check) are also used in this study. What is the difference between using 20 and 45 sites, if they both intent to represent a “global situation”.

Author Response. *To clarify, only two models overlap with the current study (SEBS and PT-JPL). The Penman-Monteith model was a single-source approach. Regardless, there are considerable advances in this current contribution. Most notably, the present study focuses on the scaling between the tower and the overlying grid, which is a critical scale of understanding in assessing the quality of our global ET estimates (for additional details, see our more detailed response in reply to Comment 1). In terms of more specific differences, the study of Ershadi et al. (2014) focused solely on a tower-based comparison of four evaporation models. Here we extend the analysis to include more than double the number of towers, an analysis encompassing a longer time period, and also examine a range of additional biome types as well as climate zones.*

Comment 3. On to content there is not much difference between the two studies, given that the grid-box scale evaluation performed here is not valid. Moreover, these two studies even come to a similar conclusion that PT-JPL seems to perform generally better than the other models.

Author Response. *We completely disagree with the reviewers position that the grid-scale evaluation is invalid. Apart from providing no justification for such a statement, the reviewer offers no alternative approach to evaluating global flux simulations (despite recognizing the importance of such research). In terms of the many differences between the works, as well as the fundamental scientific rationale which differentiates these, we refer the reader to our previous responses to Comments 1 and 2. That the papers arrive at a similar conclusion is a verification of the robustness of findings from the earlier work: a very appropriate outcome.*

Comment 4. Page 6823-Line 1. Soil evaporation in PM-MU is not entirely based on the Penman-Monteith equation, although it uses PM to estimate potential ET over unsaturated surface. Then, the effects of soil moisture restriction on soil evaporation are reflected by meteorological forcing based on the complementary relationship.

Author Response. *The reviewer is correct in that PM-Mu used a hybrid approach to soil evaporation. Specifically, the PM-Mu actual soil evaporation flux is calculated using potential soil evaporation and a soil moisture constraint function from the Fisher et al. (2008) ET model. This function is based on the complementary hypothesis (Bouchet, 1963), which defines land-atmosphere interactions from air VPD and relative humidity (RH, %). The paper has been modified to reflect this. We had deliberately minimised model descriptions, given the large body of literature available to these models, but have adjusted the text to reflect these additional details.*

Author Changes: *We have changed the relevant lines in Section 2.2.3 to reflect the following: "Estimation of evaporation for the interception and transpiration components is based on the Penman-Monteith equation (Monteith, 1965). Actual soil evaporation is calculated using potential soil evaporation and a soil moisture constraint function from the Fisher et al. (2008) ET model. This function is based on the complementary hypothesis (Bouchet, 1963), which defines land-atmosphere interactions from air VPD and relative humidity (RH, %). Evaporation components are weighted based on the fractional vegetation cover, relative surface wetness and available energy."*

Comment 5. Page 6824-Line 25. Ep is the annual potential evaporation.

Author Response. *Noted. Thanks for this editorial correction.*

Author Changes. *The sentence has now been changed to state potential evaporation.*

Comment 6. The PM-Mu model was designed to run at a time scale longer than a day, and so the model parameters were calibrated at that time scale. If using the default parameter value at the instantaneous time scale, there can be some uncertainties. This issue needs to be mentioned and discussed.

Author Response. *In the PM-MU (MOD-16) ATBD document it is stated: “The MOD16 algorithm computes ET at a daily time step. This is made possible by the daily meteorological data, including average and minimum air temperature, incident PAR and specific humidity, provided by NASA’s Global Modeling and Assimilation Office (GMAO or MERRA GMAO)”. If this is the case, one assumes that the parameters used are appropriate for that time scale. It is worth noting that the developer of the model (Qiaozhen Mu) is a co-author on a related publication where the model is used at the 3-hourly time scale! Nonetheless, the possible influence of parameter specification has now been mentioned explicitly at the end of Section 2.2.3.*

Author Changes. *Lines added at the end of Section 2.2.3. “One consideration that may influence model simulations is that this parameterization approach was developed at the daily-scale. However, both the present and also a recent related study (Miralles et al. 2015) suggest no obvious impact for sub-daily application.”*

Comment 7. Page 6826-Line6. Figure 4 should be Figure3.

Author Response. *Noted. Thanks for this editorial correction.*

Author Changes. *The sentence has been adjusted to refer to Figure 3.*

Comment 8. Page 6826-Line13-15. This is not supervising, because primary use of meteorological data does not allow PM-Mu to effectively capture the soil moisture restriction on ET on a physical basis. The consequences of that are a slower response of variations in energy and heat fluxes than the thermal remote sensing-based ET models and unreasonable spatial ET patterns (because the spatial variation in soil moisture is usually much larger than that in climate variables and vegetation types).

Author Response. *It is unclear what the reviewer wishes to convey in this comment, particularly in regards to “supervising”. In terms of the PM-Mu approach, we have not previously observed (or are aware of) any inferred lag in response. Similarly, no such lag has been observed in either PT-JPL or SEBS in a number of intercomparison exercises. Only GLEAM makes explicit use of a soil moisture term: none of the other models incorporate moisture dynamics.*

Comment 9. Line 6827-Line 15. Why the aridity index varies between 0 to 1? P can be larger than Ep, for example, in Amazon.

Author Response. *The author is correct in that the aridity index can go beyond a value of 1. As we are not exploring the concept of aridity in tropical environments, we had limited the scale to fall between 0-1. The purpose of this overlay was to show the performance of the models in dryer-conditions. I would note that the maximum value is 2.16. To avoid any potential confusion, we have adjusted the secondary axis to vary between 0-2 to better reflect the full range of aridity values.*

Author Changes. *Figures have been updated to reflect the full range of aridity index (varying between 0-2) and have been placed on a secondary y-axis (to remove the 0-1 range conflict with the r statistic)*

Comment 10. Page 6835-Line 24. I am not sure if the performance of SEBS is that highly dependent on vegetation height. As shown in this study, SEBS also fails in estimating ET over shrubland, where vegetation height is generally low (shorter than 3 m). To me, the key issue here is single-source vs multi-source. SEBS is a single source model that does not allow partitioning between soil evaporation and plant transpiration. In shrubland ecosystems where vegetation cover is usually low and highly non-uniform, soil evaporation account for a large proportion of the total ET. In this case, I would expect that SEBS overestimates ET, as demonstrated by the authors. Similar conclusion was made in a comparison study by Choi et al. (2009), in which they found that multi-source models consistently outperform single-sources models, and the largest discrepancy was found in areas with LAI smaller than 2 (indicate low vegetation cover and possibly non-uniform cover).

Author Response. *The reviewer offers some excellent additional insight into the SEBS model. However, it is worth noting that Choi et al. (2009) did not specifically study the SEBS model, so it is hard to draw definitive conclusions as to that studies translation to the present work, particularly as it focused only on corn and soybean agricultural fields (i.e. croplands in our study). But the reviewers point remains, although not necessarily in the manner described: in a recent study focusing on the Penman-Monteith model (Ershadi et al. 2015), a single-source PM model outperformed other dual and three source configurations over grasslands and shrublands, highlighting the complexity of these interactions as well as model specific performance.*

Choi, M., W. P. Kustas, M. C. Anderson, R. G. Allen, F. Li, and J. H. Kjaersgaard (2009) "An intercomparison of three remote sensing-based surface energy balance algorithms over a corn and soybean production region (Iowa, U.S.) during SMACEX", Agr. Forest Meteorol., 149, 2082–2097, doi:10.1016/j.agrformet.2009.07.002.

Comment 11. Page 6840-Line10. While I tend to agree that coarse resolution meteo files will reduce the model performance, I do not see this point is well supported by the analysis here. Again, this is due to inappropriate validation of 0.5 degree ET estimates by using 1~2 km² flux-tower observation. This is wrong.

Author Response. *The analysis performed here could not be more conclusive that simulations using the coarse-resolution forcing data perform worse than simulations run with the corresponding tower data. In the absence of other performance metrics, the tower fluxes offer an appropriate means through which to assess model behavior. Indeed, this is a standard approach, so it is unclear precisely what the reviewer is challenging here. We are afraid that this issue must remain a matter of opinion, because we cannot see a way of substantiating your argument without having validation data at 0.5 degrees resolution (and of course if we did have those data, the disagreement would not be unnecessary). These points are well explained throughout the Discussion section.*

The GEWEX LandFlux project: evaluation of model evaporation using tower-based and globally-gridded forcing data

Matthew F. McCabe^{1*}, Ali Ershadi¹, Carlos Jimenez², Diego G. Miralles³, Dominik Michel⁴ and Eric F. Wood⁵

[1] {Division of Biological and Environmental Sciences and Engineering, King Abdullah University of Science and Technology, Thuwal, Saudi Arabia}

[2] {Estellus, Paris, France}

[3] {Department of Earth Sciences, VU University Amsterdam, Amsterdam, The Netherlands}

[4] {Institute for Atmospheric and Climate Sciences, ETH Zurich, Zurich, Switzerland}

[5] {Department of Civil and Environmental Engineering, Princeton University, Princeton, United States of America}

* Correspondence to: matthew.mccabe@kaust.edu.sa

Abstract

Determining the spatial distribution and temporal development of evaporation at regional and global scales is required to improve our understanding of the coupled water and energy cycles and to better monitor any changes in observed trends and variability of linked hydrological processes. With recent international efforts guiding the development of long-term and globally distributed flux estimates, continued product assessments are required to inform upon the selection of suitable model structures and also to establish the appropriateness of these multi-model simulations for global application. In support of the objectives of the GEWEX LandFlux project, four commonly used evaporation models are evaluated against data from tower-based eddy-covariance observations, distributed across a range of biomes and climate zones. The selected schemes include the Surface Energy Balance System (SEBS) approach, the Priestley-Taylor Jet Propulsion Laboratory (PT-JPL) model, the Penman-Monteith based Mu model (PM-

27 | Mu) and the Global Land Evaporation Amsterdam Model (GLEAM). Here we seek to examine
28 | the fidelity of global evaporation simulations by examining the multi-model response to varying
29 | sources of forcing data. To do this, we perform parallel and collocated model simulations using
30 | tower-based data together with a global-scale grid-based forcing product. Through quantifying
31 | the multi-model response to high-quality tower data, a better understanding of the subsequent
32 | model response to coarse-scale globally gridded data (that underlies the LandFlux product) can
33 | be obtained, while also providing a relative evaluation and assessment of model performance.

34 | Using surface flux observations from forty-five globally distributed eddy-covariance stations as
35 | independent metrics of performance, the tower-based analysis indicated that PT-JPL provided
36 | the highest overall statistical performance (0.72 ; 61 W.m^{-2} ; 0.65), followed closely by GLEAM
37 | (0.68 ; 64 W.m^{-2} ; 0.62), with values in parenthesis representing the R^2 , RMSD and Nash-Sutcliffe
38 | Efficiency (NSE), respectively. PM-Mu (0.51 ; 78 W.m^{-2} ; 0.45) tended to underestimate fluxes,
39 | while SEBS (0.72 ; 101 W.m^{-2} ; 0.24) overestimated values relative to observations. A focused
40 | analysis across specific biome types and climate zones showed considerable variability in the
41 | performance of all models, with no single model consistently able to outperform any other.
42 | Results also indicated that the global gridded data tended to reduce the performance for all of
43 | the studied models when compared to the tower data, likely a response to scale mismatch and
44 | issues related to forcing quality. Rather than relying on any single model simulation, the spatial
45 | and temporal variability at both the tower- and grid-scale highlighted the potential benefits of
46 | developing an ensemble or blended evaporation product for global scale LandFlux applications.
47 | Challenges related to the robust assessment of the LandFlux product are also discussed.

48

49 | 1 Introduction

50 | Characterizing the exchange of water between the land surface and the atmosphere is a topic
51 | of multi-disciplinary interest, as the processes that comprise this dynamic cycling of water
52 | determine the spatial and temporal variability of hydrological responses across local and global
53 | scales. In recent years, there has been significant progress in the development of regional and
54 | global datasets based largely on remote sensing retrievals. These data have provided a wealth

Matthew McCabe 10/12/2015 10:29 AM

Deleted: : the

Matthew McCabe 10/12/2015 10:29 AM

Deleted: ethodology

Matthew McCabe 13/12/2015 1:18 PM

Deleted: and

58 of spatially and temporally varying information across a range of Earth system processes,
59 including soil moisture (Liu et al., 2011a), vegetation change (Tucker et al., 2005; Liu et al.,
60 2011b; Liu et al., 2013), groundwater (Famiglietti et al., 2011; Richey et al., 2015) and
61 precipitation (Huffman et al., 1995; Nesbitt et al., 2004), enabling a capacity to enhance our
62 understanding and description of regional- and global-scale water cycles and their spatial and
63 temporal variability. While evaporation represents the key process returning the Earth's surface
64 water to the overlying atmosphere and provides the linking mechanism between the water and
65 energy cycles, it is only in relatively recent times that effort has been directed towards the
66 development of global products (Mu et al., 2007; Fisher et al., 2008; Vinukollu et al., 2011a).

67 To address this observation limitation, a number of evaporation modelling approaches have
68 been developed over the past few years to enable estimation at scales beyond the field, using
69 satellite remote sensing (Sheffield et al., 2010; Miralles et al., 2011a) and other data sources
70 (Douveille et al., 2013). The models tend to differ in their level of empiricism and in the desired
71 scale of application, with some exclusively developed for farm-scale operation and requiring
72 local calibration (Bastiaanssen et al., 1998; Allen et al., 2007). Others have been developed for
73 broader scale application and are built on physical relationships describing the water and
74 energy transfer at the land surface (Norman et al., 1995; Su, 2002; Fisher et al., 2008; Miralles
75 et al., 2011a). While traditional applications of evaporation estimates have been directed
76 towards agricultural monitoring (Allen, 2000), catchment water budgets and basin-scale water
77 management (Kustas et al., 1994; Granger, 2000), more recent applications of evaporation
78 products have included detection and prediction of heatwaves (Hirschi et al., 2011; Miralles et
79 al., 2014a), droughts (Mu et al., 2012; Otkin et al., 2014) and in resolving the likely contribution
80 of human-induced climate change on such events (Greve et al., 2014).

81 Despite the importance of understanding the magnitude and spatial and temporal variability of
82 evaporation, the availability of long-term products required to do this are rather limited.
83 Characterizing the long-term trends and variability in independent observations of the Earth's
84 coupled water and energy cycles is a key objective of the World Climate Research Programmes
85 (WCRP) Global Energy and Water Cycle Exchanges (GEWEX) project. Towards this task, the
86 GEWEX Data and Assessments Panels (GDAP) LandFlux project has coordinated two interrelated

Matthew McCabe 13/12/2015 1:20 PM

Deleted: for

Matthew McCabe 13/12/2015 1:20 PM

Deleted: represents

89 research efforts that seek to: i) intercompare long-term gridded surface flux data sets and
90 identify their skill and reliability (i.e. product-benchmarking), and ii) simulate and intercompare
91 evaporation models to identify algorithms appropriate for developing a global flux product (i.e.
92 model-benchmarking). In one of the first global-scale product assessments, Jiménez et al.
93 (2011) examined twelve evaporation products obtained from satellite-based, reanalyses and
94 off-line LSM simulations for a 3 year period (1993-1995), identifying large correlations between
95 the products, similarity in their spatial distributions, as well as large absolute differences in the
96 annual average evaporation. A complementary investigation of the inter-product differences
97 was undertaken by Mueller et al. (2011), which included forty-one global evaporation data sets
98 across a range of satellite-based simulations, LSMs, Global Circulation Models (GCMs),
99 atmospheric reanalyses datasets, empirical up-scaling of eddy-covariance measurements, as
100 well as atmospheric water budget data sets. In that study, Mueller et al. (2011) used seven
101 years of monthly mean data for the period 1989-1995 and found strong similarity in the
102 absolute magnitude and spatial distribution of evaporation amongst the products. More
103 recently, Mueller et al. (2013) examined multi-annual trends and variations in evaporation
104 products from a range of diagnostic data sets, LSMs and reanalysis products and showed
105 consistency in inter-annual variations of evaporation products that corresponded well with
106 previous investigations (Jung et al., 2010).

107 These benchmarking studies provided a thorough (and much needed) assessment of available
108 global evaporation products and the varying approaches used to derive them. However,
109 evaluation of the models for their predictive skill was challenging due to inconsistencies in the
110 forcing data used to drive the models, as well as to the different parameterization schemes
111 employed. That is, the analysis was performed on the published evaporation output, rather
112 than re-running simulations from a common forcing dataset. In these benchmarking studies,
113 the evaporation data sets were also aggregated to similar spatial and temporal resolutions for a
114 common analysis period, to enable unbiased comparison. Uncertainties emerging from such
115 aggregations can often reduce the confidence in any such model performance ranking. One
116 initial effort addressing this was the study of Vinukollu et al. (2011a), which used the Surface
117 Energy Balance System (SEBS) model (SEBS; Su, 2002), a two-source Penman-Monteith scheme

118 by Mu et al. (2007) and a three-source model based on parameterizing the Priestley-Taylor
119 model (PT-JPL) (Fisher et al., 2008) to estimate global evaporation for the period 2003-2004.
120 The Vinukollu et al. (2011a) analysis revealed that the modelled instantaneous evaporation
121 (coinciding with the time of satellite overpass) was in reasonable agreement with locally-
122 observed evaporation at twelve eddy-covariance towers across the United States, with
123 correlations ranging from 0.43 to 0.54. However, uncertainties resulting from scale mismatch
124 between satellite data and the validation tower footprint reduced the confidence and skill
125 ranking of the models. One of the unique aspects of the present study is that tower data are
126 consistent across all model simulations: that is, tower-bias is minimized, by ensuring that all
127 models are assessed against the same tower records. Further, even though sub-grid scale
128 variability is not explored here (since none of the models explicitly account for this), the tower-
129 to-grid scale analysis acts as a diagnostic of representativeness and point-to-pixel error.

130 Recently, Ershadi et al. (2014) examined a number of models including SEBS, PT-JPL, the
131 Advection-Aridity model of Brutsaert and Stricker (1979) and a single-source Penman-Monteith
132 (PM) model (Monteith, 1965), using a set of twenty flux towers distributed across a range of
133 biome types and climate zones to force the models with tower-based data directly. Based on
134 common forcing and considering overall results, the study found that PT-JPL was the best
135 performing model, followed by SEBS, PM and Advection-Aridity. In a related contribution,
136 Ershadi et al. (2015) provided a more focused analysis on the influence of model structure and
137 resistance parameterization on single, two-layer and three-source Penman-Monteith models.
138 The authors identified considerable variability in the performance of models due to their
139 structure and parameterization choices.

140 A parallel effort to the LandFlux project is the European Space Agency (ESA) funded WAter
141 Cycle Multi-mission Observation Strategy for EvapoTranspiration (WACMOS-ET; see
142 <http://wacmoset.estellus.eu/>). WACMOS-ET, which is focused on an analysis period covering
143 2005-2007, seeks to better understand the impacts of model structure on flux estimation, with
144 an additional focus on developing a consistent forcing dataset using predominantly European
145 Space Agency developed products. A key result from these early works and the preliminary
146 outcomes from WACMOS-ET support the finding that no single model or parameterization

147 consistently outperformed any other across different biomes. [Further details on these](#)
148 [complimentary efforts can be found in Michel et al. \(2015\) and Miralles et al. \(2015\).](#)

149 While establishing a baseline level of performance at the tower scale is important,
150 understanding the impact of using the large-scale globally-gridded forcing that will ultimately
151 drive the global products is key. The focus of the current investigation is to build upon these
152 past efforts and complement ongoing WACMOS-ET investigations, by simulating state-of-the-
153 art evaporation models using a parallel assessment of tower-based meteorology and gridded
154 data, and comparing results with available eddy-covariance flux observations. Understanding
155 how application of gridded forcing data might influence the performance of the different
156 models, relative to their performance when forced with (presumably) higher-quality tower
157 data, is a motivating rationale for this work. Such evaluations are important in developing
158 insight into the sensitivity of the models to input data uncertainties, provide a relative
159 assessment of model quality and also inform upon issues of spatial scale and footprint
160 mismatch (McCabe and Wood, 2006). Establishing model suitability for large-scale operational
161 application as part of the GEWEX Landflux project is a further motivating goal for this work. As
162 such, a major objective is to evaluate the individual model responses across a range of biomes
163 and climate zones. The models selected for assessment include SEBS, PT-JPL, the Penman-
164 Monteith based Mu model (PM-Mu) (Mu et al., 2011) as well as the Global Land Evaporation
165 [Amsterdam Methodology \(GLEAM\) \(Miralles et al., 2011a\)](#). These models satisfy [a number of](#)
166 [criteria that were considered important](#) for global model selection, [including](#) reliance on a
167 minimum number of forcing variables, capacity to use remote sensing based observations, as
168 well as previous application at either the regional or global scale.

169

170 2 Data and Methodology

171 2.1 Data

172 For this analysis, model simulations cover the period from 1997 to 2007 and are performed at a
173 3-hourly temporal resolution. To examine model response and inter-product variability, a

Matthew McCabe 10/12/2015 10:28 AM

Deleted: :

Matthew McCabe 10/12/2015 10:28 AM

Deleted: the

Matthew McCabe 13/12/2015 1:31 PM

Deleted: the key

Matthew McCabe 13/12/2015 1:31 PM

Deleted: which

Matthew McCabe 13/12/2015 1:31 PM

Deleted: ed

179 parallel tower- and grid-based analysis was performed. Data for the tower-based analysis are
180 derived from a set of forty-five eddy-covariance towers (see [Table A1](#)), while the gridded data
181 are extracted from a compilation of available globally distributed satellite, meteorological and
182 land surface characteristics products. Compared to the 0.5 degree and 3-hourly gridded data,
183 the use of tower-based forcing is expected to minimize issues related to footprint uncertainties
184 when evaluating simulations against the observed eddy-covariance based flux data. The
185 primary purpose of the grid-based analysis is to better understand the effects of large-scale
186 forcing data on the accuracy of global retrievals, relative to the tower-based evaluations.

Matthew McCabe 13/12/2015 4:09 PM
Deleted: Table A1

187 2.1.1 Description of tower-based forcing data

188 Data for the tower-based analyses are derived from forty-five eddy-covariance towers selected
189 from within the FLUXNET database (Baldocchi et al., 2001). [Table A1](#) lists the key attributes of
190 the selected towers and [Figure A1](#) describes the varying temporal lengths of the tower records
191 used in this study. The requirement that towers only be used if they are able to provide the
192 input data required by all models (see Table 1) was a strong limiting criterion that significantly
193 reduced the number of available study sites. In particular, the availability of land surface
194 temperature data, which is required for SEBS, drastically constrained the choice of towers.
195 However, ensuring data consistency within the towers used for simulation and assessment was
196 an important component of this work, as it removes the impact of tower bias in subsequent
197 model assessment. Even with this reduced number, the selected towers represent a
198 considerable spatial spread encompassing a variety of biome types and climate zones (see
199 Figure 1).

Matthew McCabe 13/12/2015 4:09 PM
Deleted: Table A1

Matthew McCabe 13/12/2015 4:09 PM
Deleted: Figure A1

200 In terms of forcing data requirements, tower-based variables that were used for model
201 simulations include air temperature, relative humidity, wind speed, net radiation, ground heat
202 flux and precipitation. A summary of the forcing data requirements for each model is provided
203 in Table 1. Land surface emissivity, leaf area index and fractional vegetation cover were
204 estimated from Normalized Difference Vegetation Index (NDVI) data obtained from the Global
205 Inventory Monitoring and Modelling Study (GIMMS) dataset (Tucker et al., 2005), at 8 km
206 spatial and bi-monthly temporal resolutions. Here, the emissivity was calculated using the

210 approach of Sobrino et al. (2004), leaf area index was estimated following Fisher et al. (2008)
211 and the fractional vegetation cover was estimated using the technique described in Jiménez-
212 Muñoz et al. (2009). Land surface temperature was calculated using tower-observed longwave
213 upward radiation and by inverting the Stefan-Boltzmann equation (Brutsaert, 2005).
214 Atmospheric pressure data, which are absent from many towers, were calculated based on
215 ground elevation of tower locations using an equation presented in Bos et al. (2008). Canopy
216 height (h_c), which is needed for the SEBS model, was obtained from tower metadata and was
217 assumed constant during the simulation period. Although h_c varies over many vegetation types,
218 accounting for its within- and inter-annual variability is usually not possible, as observed data of
219 h_c variations are rarely recorded. Tower data were aggregated (i.e. summed for precipitation
220 and averaged for other input variables) from their native resolution of half-hourly or hourly to
221 3-hourly, to match the temporal resolution of the gridded data.

222 2.1.2 Description of grid-based forcing data (LandFlux Version 0 forcing dataset)

223 Grid-based data were developed by Princeton University for the LandFlux Version 0 (V-0)
224 dataset. The variables in the V-0 include air temperature, land surface temperature, wind
225 speed, atmospheric pressure, specific humidity, precipitation, net radiation, NDVI and leaf area
226 index. Net radiation data derive from the GEWEX Surface Radiation Budget (SRB) Version-3
227 (Stackhouse et al., 2011), while land surface temperature is determined by employing a
228 Bayesian post-processing procedure that merges High-Resolution Infrared Radiation Sounder
229 (HIRS) retrievals with the land surface temperature data from the National Centers for
230 Environment Prediction (NCEP) Climate Forecast System Reanalysis (CFSR) (Saha et al., 2010), as
231 described in Coccia et al. (2015). Precipitation data are also from the NCEP CFSR product and
232 have been bias-corrected to the Global Precipitation Climatology Project (GPCP) V2.2 dataset
233 (Adler et al., 2003). Likewise, atmospheric pressure, specific humidity and wind speed data
234 were extracted from the CFSR reanalysis data. For vegetation based parameters, NDVI data
235 were prepared by aggregating 8-km resolution GIMMS NDVI data to 0.5° resolution, while leaf
236 area index data were developed by Zhu et al. (2013) through fitting GIMMS NDVI data to the
237 Moderate Resolution Imaging Spectroradiometer (MODIS) MOD15A2 NDVI product, using a
238 neural network technique.

Matthew McCabe 13/12/2015 1:34 PM

Deleted:

Matthew McCabe 13/12/2015 1:34 PM

Deleted: short

Matthew McCabe 13/12/2015 1:09 PM

Deleted: A recent global sensitivity analysis of the SEBS model (Ershadi and McCabe, 2015), showed that h_c was amongst the least sensitive variables in SEBS, reducing concerns on the impact of this assumption.

Matthew McCabe 13/12/2015 1:39 PM

Deleted: A

Matthew McCabe 13/12/2015 1:39 PM

Deleted: also based

Matthew McCabe 13/12/2015 1:39 PM

Deleted: on

249 The majority of variables in the global LandFlux V-O forcing dataset are at 0.5° spatial and 3-
 250 hourly temporal resolution. Exceptions include the net radiation (1° and 3-hourly), NDVI (0.5°
 251 and bi-monthly) and leaf area index (0.5° and monthly). For net radiation, the 1° data were
 252 linearly interpolated to a 0.5° resolution. The bi-monthly NDVI data were assumed constant for
 253 all 3-hourly time steps during each 15-day interval, while the leaf area index data were assumed
 254 constant during each month. The canopy height over shrubland and forest biomes was
 255 assumed fixed and was estimated using a static canopy height product developed by Simard et
 256 al. (2011). For grassland and cropland biomes, where the dynamics of canopy height can be
 257 considerable, canopy height was calculated using Equation 1, derived from Chen et al. (2012):

$$258 \quad h_c = h_c^{min} + \frac{h_c^{max} - h_c^{min}}{NDVI_{max} - NDVI_{min}} \times (NDVI - NDVI_{min}) \quad (1)$$

259 where h_c^{min} and h_c^{max} are the minimum and maximum canopy height and were obtained from
 260 the static vegetation table of the North American Data Assimilation System (NLDAS) (available
 261 from <http://ldas.gsfc.nasa.gov/nldas/web/web.veg.table.html>). $NDVI_{min}$ and $NDVI_{max}$ are the
 262 minimum and maximum NDVI, respectively, and were calculated on a pixel-wise basis for each
 263 calendar year. The JPL static vegetation height was aggregated linearly from 1 km to 0.5°.
 264 Likewise, the NDVI derived canopy height was calculated at 8 km resolution and then
 265 aggregated to 0.5°. Similar to the tower-based data, the methodology of Jiménez-Muñoz et al.
 266 (2009) was used for the gridded forcing to estimate the fractional vegetation cover data from
 267 NDVI data. The ground heat flux at the grid-scale was calculated as a fraction of net radiation
 268 using fractional vegetation cover, following Su (2002).

269 2.1.3 Model specific forcing data and data sources

270 In addition to the data described above and shown in Table 1, both GLEAM and SEBS have some
 271 model specific forcing data requirements. For SEBS, information on land surface temperature,
 272 wind-speed and canopy height are required. At the tower-scale, these data are provided by
 273 available meteorological forcing or meta-data descriptions in the case of canopy height. At the
 274 grid-scale they are provided by a combination of the LandFlux V-O dataset and an adapted JPL
 275 static vegetation height, as described in Section 2.1.2. GLEAM based simulations require

Matthew McCabe 13/12/2015 2:02 PM

Deleted: onto

Matthew McCabe 13/12/2015 2:02 PM

Deleted: s

278 information on soil properties, vegetation optical depth (VOD), satellite soil moisture, snow
279 water equivalent, lightning frequency and vegetation cover fraction. Soil properties data for
280 GLEAM include field capacity, critical soil moisture and wilting point soil moisture thresholds.
281 Data for these were obtained from the Global Gridded Surfaces of Selected Soil Characteristics
282 dataset of the International Geosphere-Biosphere Programmes Data and Information System
283 (IGBP-DIS), available from Oak Ridge National Laboratory Distributed Active Archive Center
284 (<http://www.daac.ornl.gov>). Soil properties data were used in their native 5 arc-minute
285 resolution for tower-based analysis, but were aggregated to 0.5° for grid-based assessment.
286 Vegetation optical depth data was from Liu et al. (2011b) using a merged product from multiple
287 microwave based satellite data. The 0.25° spatial and daily temporal resolutions VOD data were
288 gap-filled as described by Miralles et al. (2011a). Soil moisture data assimilated in GLEAM
289 comes from the CCI-WACMOS dataset (Liu et al., 2012) produced from both active and passive
290 satellite microwave data at 0.25° and daily resolution. Snow water equivalent data are from the
291 GlobSnow product version 1.0 (Luo et al., 2010); as GlobSnow covers the northern
292 hemisphere only, Global Monthly Snow Water Equivalent Climatology data from the National
293 Snow and Ice Data Center (NSIDC) (Armstrong et al., 2005) are used for the BW-Ma1 tower (see
294 [Table A1](#)) located in the southern hemisphere. Both GlobSnow data and the NSIDC product are
295 at approximately 0.25° spatial and daily temporal resolutions. Lightning frequency data is based
296 on the Combined Global Lightning Flash Rate Density monthly climatology at 0.5° (Mach et al.,
297 2007) and it is used to calculate a climatology of rainfall rates (Miralles et al., 2010). Finally,
298 vegetation cover fractions are derived from the MODIS MOD44B product (Hansen et al., 2005).
299 The MODIS continuous cover fractions describe every pixel as a combination of its fractions of
300 water, tall canopy, short vegetation and bare soil. The temporal average of fractions is used
301 here for the MODIS period, providing only a static cover fraction for the GLEAM simulations.
302 The MOD44B product is available at 250 m and 0.25° resolution. For tower-based analysis,
303 cover fractions are at 250 m resolution, but for grid-based analysis the 0.25° MOD44B product
304 was aggregated to 0.5°.

305 [Table 1](#) summarizes the different sources and spatio-temporal scales of the data that were used
306 for both the tower- and grid-based flux simulations. As noted earlier, the temporal analysis

Matthew McCabe 13/12/2015 4:09 PM
Formatted: Font:Not Italic, Check spelling and grammar

Matthew McCabe 13/12/2015 4:09 PM
Deleted: Table A1

Matthew McCabe 13/12/2015 4:09 PM
Deleted: Table 1

Matthew McCabe 13/12/2015 2:07 PM
Formatted: Font:Not Italic

Unknown
Field Code Changed

309 encompasses the period 1997-2007, although as defined in Figure A1, the individual tower
310 records do not necessarily provide uninterrupted observations during this time range.

311 2.1.4 Definition of selected biome type and climate zones

312 The specific biomes examined in this work include wetland (WET), grassland (GRA), cropland
313 (CRO), shrubland (SHR), evergreen needleleaf forest (ENF), evergreen broadleaf forest (EBF) and
314 deciduous broadleaf forest (DBF). Biome type was specified in Fluxnet metadata records for
315 each of the individual tower sites and follows the International Geosphere-Biosphere
316 Programme (IGBP) classification. For simplicity, the shrubland biome is comprised of closed
317 shrubland, woody savannah and mixed forest biomes. The number of towers for each biome
318 type varies, with fourteen for evergreen needleleaf forest, ten for grassland, seven for
319 cropland, seven for deciduous broadleaf forest, four for shrubland, two for wetland and only
320 one for evergreen broadleaf forest (see Table A1). The climate zones include boreal (BOR), sub-
321 tropical (subTRO), temperate (TEMP), temperate-continental (TempCONT) and dry (DRY) for
322 arid and semi arid regions. These zones were prescribed from the tower specific metadata,
323 which were in turn derived from Rubel and Kottek (2010), based on a Köppen-Geiger climate
324 classification. As with biome type, the towers are not evenly distributed across climate zones,
325 with fifteen for temperate, eleven for sub-tropical, eight for temperate-continental, five for
326 boreal and six for dry regions (see Table A1).

327 2.2 LandFlux Model Descriptions

328 Following are brief descriptions of the models employed in this analysis. For a more
329 comprehensive explanation of the implementation of these different schemes, the reader is
330 referred to the principal model references as well as the recent contributions of Ershadi et al.
331 (2014) and Ershadi et al. (2015).

332 2.2.1 SEBS

333 SEBS is a widely employed process-based model used in the estimation of evaporation. The
334 model uses a variety of land surface and atmospheric variables and parameters for simulating
335 the transfer of heat and water vapor from the land surface to the atmosphere. To do so, the

Matthew McCabe 10/12/2015 11:00 AM
Formatted: Left

Matthew McCabe 13/12/2015 4:09 PM
Formatted: Font:Not Italic, Check spelling
and grammar

Matthew McCabe 13/12/2015 4:09 PM
Deleted: Table A1

Matthew McCabe 13/12/2015 4:09 PM
Formatted: Font:Not Italic, Check spelling
and grammar

Matthew McCabe 13/12/2015 4:09 PM
Deleted: Table A1

Matthew McCabe 13/12/2015 1:15 PM
Deleted: -

model first estimates the representative roughness of the land surface and then uses roughness parameters, temperature gradient and wind speed data to estimate sensible heat flux via a set of flux-gradient equations describing the transfer of heat from the land surface to the atmosphere. Depending on the atmospheric boundary layer height, the model uses either the Monin-Obukhov Similarity Theory or the Bulk Atmospheric Similarity Theory equations (Brutsaert, 2005). The model estimates the sensible heat flux of hypothetically wet and dry conditions and uses these extreme-cases to calculate the evaporative fraction. Evaporation is then calculated as a fraction of the available energy. The model requires accurate values of net radiation, land surface temperature, air temperature, humidity, wind speed and vegetation phenology to calculate surface fluxes. SEBS relaxes the need for parameterization of the surface resistance, but is sensitive to aerodynamic resistance parameterization (Ershadi et al., 2013). Further details on SEBS and its model formulation can be found in Su (2002).

2.2.2 PT-JPL

The PT-JPL model of evaporation uses a minimum of meteorological and remote sensing data and has been employed in a number of studies to estimate regional and global scales flux response (Fisher et al., 2008; Sahoo et al., 2011; Vinukollu et al., 2011b; Vinukollu et al., 2011a; Badgley et al., 2015). A key characteristic of the model is the use of bio-physiological properties of the land surface to reduce Priestley-Taylor potential evaporation to actual values. The PT-JPL is a three source model in which the total evaporation is partitioned into soil evaporation (λE_s), canopy transpiration (λE_t), and wet canopy evaporation (λE_i), i.e. $\lambda E = \lambda E_s + \lambda E_t + \lambda E_i$. The model first partitions the total net radiation to soil and vegetation components and calculates potential evaporation for soil, for canopy and for the wet canopy. The model then determines a set of constraint multipliers to represent the impacts of green canopy fraction, relative wetness of the canopy, air temperature, plant water stress and soil water stress on the evaporative process. The model uses the constraint multipliers to reduce the potential evaporation to actual values for each component of the system. PT-JPL does not calibrate or tune parameter values and does not use wind speed data or parameterizations of the aerodynamic and surface resistances. However, the model does require accurate estimates of optimum temperature

367 | (T_{opt}) (Potter et al., 1993) for canopy transpiration. The optimum temperature is the air
368 | temperature at the time of peak canopy activity, when the highest values of absorbed
369 | photosynthetically active radiation and minimum values of vapour pressure deficit occur.
370 | Further details of the PT-JPL model can be found in Fisher et al. (2008).

371 | 2.2.3 PM-Mu

372 | The PM-Mu was expanded from a two-source Penman-Monteith implementation (Mu et al.,
373 | 2007) to a three-source version (Mu et al., 2011), which forms the basis behind the near real-
374 | time estimation of global evaporation in the MOD16 product (Mu et al., 2013), (n.b. the PM-Mu
375 | nomenclature used herein reflects an identical description used in Michel et al. (2015) and
376 | Miralles et al. (2015), where it is referred to as PM-MOD). Evaporation in the PM-Mu model is
377 | the sum of soil evaporation, canopy transpiration and evaporation of the intercepted water in
378 | the canopy, i.e. ($\lambda E = \lambda E_s + \lambda E_t + \lambda E_i$). Estimation of evaporation for interception and
379 | transpiration components is based on the Penman-Monteith equation (Monteith, 1965). Actual
380 | soil evaporation is calculated using potential soil evaporation and a soil moisture constraint
381 | function from the Fisher et al. (2008) ET model. This function is based on the complementary
382 | hypothesis (Bouchet, 1963), which defines land-atmosphere interactions from air vapour
383 | pressure deficit and relative humidity. Evaporation components are weighted based on the
384 | fractional vegetation cover, relative surface wetness and available energy. Parameterization of
385 | aerodynamic and surface resistances for each source is based on extending biome specific
386 | conductance parameters from the stomata to the canopy scale, using vegetation phenology
387 | and meteorological data. In contrast to the majority of Penman-Monteith type of models, the
388 | PM-Mu does not require wind speed and soil moisture data for parameterization of resistances.
389 | However, global application of the model requires consideration of the fact that resistance
390 | parameters were calibrated against data from a set of eddy-covariance towers. One
391 | consideration that may influence model simulations is that this parameterization approach was
392 | developed at the daily-scale. However, both the present and also a recent related study
393 | (Miralles et al. 2015) suggest no obvious impact for sub-daily application. Further details on
394 | PM-Mu can be found in Mu et al. (2011) and Mu et al. (2013).

Matthew McCabe 13/12/2015 2:15 PM

Deleted: developed

Matthew McCabe 13/12/2015 2:16 PM

Deleted: and

Matthew McCabe 10/12/2015 4:14 PM

Deleted: .

Matthew McCabe 10/12/2015 4:06 PM

Deleted: Estimation of evaporation for each component is based on the Penman-Monteith equation (Monteith, 1965), but weighted based on the fractional vegetation cover, relative surface wetness and available energy.

Matthew McCabe 13/12/2015 2:17 PM

Deleted: ly

Matthew McCabe 10/12/2015 4:14 PM

Deleted:

406 2.2.4 GLEAM

407 GLEAM (Miralles et al., 2011a) has been used not only in estimating global evaporation
408 (Miralles et al., 2011b) but also in detection and evaluation of heatwaves (Miralles et al.,
409 2014a), climate variability (Miralles et al., 2014b) and land-atmospheric feedbacks (Guilod et
410 al., 2015). Designed as a satellite data based model, GLEAM first estimates interception loss
411 using the analytical method of Gash (1979) and then applies the Priestley-Taylor equation to
412 calculate potential evaporation for soil and vegetation. Like PT-JPL, the model constrains the
413 potential evaporation values to actual values by applying a stress factor, although GLEAM is
414 based on different assumptions and encompasses both moisture availability in a multi-layered
415 soil system and vegetation water content inferred from vegetation optical depth data (Liu et al.,
416 2011b). In contrast to SEBS, PT-JPL and PM-Mu, the GLEAM model is equipped with routines to
417 quantify sublimation of snow-covered regions, to estimate open-water evaporation and to
418 assimilate remote sensing soil moisture data. Routine application of GLEAM is usually
419 performed in time-series mode, in which the model tracks the changes of soil moisture state
420 across time ~~steps~~. Here, to allow application of the model at the tower-scale, gaps in the tower
421 data were filled by establishing correlation between the variables in tower- and grid-based
422 data. Simulated evaporation values were filtered from the analysis for these gap-filled periods.
423 Further details on GLEAM can be found in Miralles et al. (2011a;b).

424 2.3 Model Simulation and Analysis

425 The four selected models were forced with both tower- and grid-based data. The results were
426 then filtered for daytime-only periods, defined as when the shortwave downward radiation
427 exceeds 20 W.m^{-2} , to avoid issues associated with negative net radiation and night_time
428 condensation. The data were also filtered for rain events, for negative sensible and latent heat
429 flux observations, for low quality or gap-filled tower records, for frozen land surfaces and for
430 times in which air temperature was less than or equal to 0°C . The performance of the models
431 was evaluated for individual towers, for the collection of data from all towers, for towers
432 classified across biome types and for towers classified across climate zones.

Matthew McCabe 13/12/2015 2:20 PM
Deleted: stamps

To evaluate the skill of the models, we used traditional scatterplots and common statistical metrics including the coefficient of determination (R^2), slope (m) and y-intercept (b) of the linear regression, the root-mean-square difference ($RMSD$), relative error [$RE = RMSD/\text{mean}(\lambda E_{obs})$] and the Nash-Sutcliffe Efficiency (NSE) (Nash and Sutcliffe, 1970). In developing these performance metrics, simulated evaporation was compared with tower-observed evaporation (λE_{obs}) that were corrected for non-closure using the energy residual technique, as described in Ershadi et al. (2014). Scatterplots of matching percentiles (referred to hereafter as percentile plots) of observed evaporation versus simulated values from the 1st to 99th percentile increment were also used (Section 3.1). The 25th percentile (Q_{25}), median (Q_{50}) and 75th percentile (Q_{75}) were used for further model assessment. To establish the response of the models to water availability at individual tower sites, we calculated an aridity index as $AI = P/E_p$, with P the annual precipitation (mm.yr⁻¹) and E_p the annual **potential** evaporation (mm.yr⁻¹), calculated using a Priestley-Taylor equation and assuming an alpha-coefficient of 1.26. LandFlux V-0 data (Section 2.1.2) at 3-hourly resolution were used to calculate aridity index values and an average value was calculated to represent the state of water availability at specific tower locations.

450

451 3 Results

452 3.1 Relative performance of the models when using tower-based and gridded data

Figure 2 and Figure 3 show scatterplots, percentile plots and relevant statistical metrics of the modelled evaporation for all of the available 3-hourly data records from across the forty-five towers (representing 115,148 records in total). For the tower-based analysis (see Figure 2), PT-JPL presents the best overall performance with lower model spread and an $RMSD = 61 \text{ W.m}^{-2}$, $RE = 0.41$, $R^2 = 0.71$ and an $NSE = 0.65$. The model slightly underestimates evaporation, with a slope of linear regression equal to 0.91 and with the majority of the percentile plot (up to Q_{75}) located just under the 1:1 line. When considering results across all towers, GLEAM presents comparable statistical performance to PT-JPL, with an $RMSD = 64 \text{ W.m}^{-2}$, $RE = 0.43$ and an $NSE = 0.62$. GLEAM tends to slightly underestimate evaporation, with the slope of linear regression

462 equal to 0.84 and with the percentile plot being located under the 1:1 line. SEBS generally
463 overestimates evaporation and has the lowest overall performance, with an $RMSD = 101 \text{ W.m}^{-2}$,
464 $RE = 0.68$ and $NSE = 0.24$, even though it has one of the highest R^2 values at 0.72. For PM-Mu,
465 the model tends to underestimates evaporation, resulting in an $RMSD = 78 \text{ W.m}^{-2}$, $RE = 0.52$
466 and an $NSE = 0.45$. Overall, the PT-JPL and GLEAM seem to present as more robust candidate
467 models for estimation of evaporation, at least in terms of their statistical response at the tower
468 scale. All models show a large spread around the fitted linear regression line, While the
469 summary statistics are useful metrics of performance, the inter-tower variability of the models
470 is an important element of this work and will be discussed further in the following sections.

Matthew McCabe 10/12/2015 11:16 AM

Deleted: , due perhaps to variability in performance as a response to the land surface type or climate condition

Matthew McCabe 13/12/2015 2:29 PM

Deleted: T

471 The effect of using globally-gridded forcing data on the evaporation models is presented in
472 Figure 3. Apart from providing a direct evaluation on the accuracy of the global LandFlux
473 product, assessing flux response to a change in forcing aids in diagnosing the model sensitivity
474 to data uncertainties (which are inherent in any data product). Likewise, an indirect assessment
475 of the issue of footprint mismatch between the gridded data (0.5°) and the eddy-covariance
476 tower (hundreds of meters) can also be inferred. Figure 3 clearly shows that use of the grid-
477 based data reduces the performance of all models relative to the tower-based runs, with all
478 statistics degrading with a change in forcing resolution. SEBS displayed the largest sensitivity to
479 forcing data, with a 0.4 decrease in NSE and a 28 W.m^{-2} increase in $RMSD$. The sensitivity of PT-
480 JPL and GLEAM to the use of gridded data was lower, with both showing an approximately 0.3
481 decrease in NSE and around 22 W.m^{-2} increase in $RMSD$ when assessing the grid-based analysis.
482 Overall, PM-Mu shows the lowest sensitivity to forcing, with a 0.26 decrease in NSE and 18
483 W.m^{-2} increase in $RMSD$, albeit presenting the lowest correlation and slope of linear regression
484 for all model responses.

Matthew McCabe 10/12/2015 4:17 PM

Deleted: 4

485 Overall, these results confirm that all models display a relatively high sensitivity to changes in
486 the type and quality of input forcing data. While gridded forcing data are expected to have a
487 mismatch with the tower-based forcing due to their larger pixel (and footprint) sizes, this
488 spatial mismatch will impact all of the applied models, albeit to a lesser or greater extent,
489 depending on forcing data requirements. While spatial scale no doubt plays a major role in
490 decreasing model efficiencies at grid-scales, a key reason for the differences in tower- versus

Matthew McCabe 13/12/2015 2:32 PM

Deleted: the most likely

497 grid-based results relates to internal inconsistencies within the gridded forcing data. For
498 instance, SEBS is known to be particularly sensitive to the temperature gradient between the
499 land surface and the atmosphere (van der Kwast et al., 2009; Ershadi et al., 2013). While the
500 temperature gradient at the tower scale is more reliable due to application of the tower-based
501 sensors for air temperature and land surface temperature, obtaining such consistency is harder
502 when different sources of forcing data are employed (see Section 2.1). Not surprisingly, results
503 also indicate that those models that use fewer inputs show lower sensitivity to changes in the
504 forcing. As such, any inconsistency between the tower and gridded data is likely to have less
505 influence on the PT-JPL, GLEAM and PM-Mu models than it will on SEBS, which in addition to
506 vegetation height, requires both land surface temperature and wind speed data: two variables
507 with considerable spatial variability. Disentangling the varying influence of model structural and
508 forcing data uncertainty requires focused attention and is examined further in the Discussion
509 section.

510 The large spread of data in the scatterplots indicates that there is considerable variability in the
511 performance of the models at individual towers, irrespective of whether tower or gridded data
512 are used. Of course, it may also be indicative of systematic biases in the in-situ data, which vary
513 from one tower to another and subsequently impact on model spread: however, this is non-
514 trivial to determine. To investigate the nature of this variability, we extend the analysis by
515 developing time series of R^2 , RE and NSE at 3-hourly resolution for individual tower locations, as
516 shown in Figure 4. To examine performance as a function of hydrological condition, the towers
517 are arranged by degree of increasing aridity, as determined by calculation of an aridity index
518 (see Section 2.3), with left-to-right representing the transition from wet-to-dry and describing
519 an aridity index varying between approximately 2 and 0.

520 From Figure 4 it can be observed that there is a general downward trend in both R^2 and NSE as
521 aridity increases, with a slight upward trend reflected in RE . In terms of R^2 , most of the models
522 (except for PM-Mu) show some consistency in performance until an aridity index of around 0.7,
523 wherein models start to diverge. Similar agreement is seen in the relative error plot, although
524 the outlier here is SEBS, which shows variable performance unrelated to aridity changes.
525 Examining the Nash-Sutcliffe efficiency allows for a clearer evaluation of model response to be

Matthew McCabe 13/12/2015 2:33 PM
Deleted: 1

527 obtained. For this metric, PT-JPL and GLEAM display relatively good correspondence for most of
528 the towers, but start to diverge more regularly for aridity indices below 0.8. Overall, PT-JPL
529 presents a marginally better response than GLEAM, with higher values of NSE and R^2 and lowest
530 values of RE produced across the majority of towers. Similar results are expressed in Figure A2,
531 which presents the same tower based inter-comparison as in Figure 4, but for the grid-scale
532 model simulations.

533 From Figure 2 it was observed that SEBS presented the lowest values of NSE and highest values
534 of RE , while PM-Mu had the lowest values of R^2 . Highlighting the importance of examining a
535 range of statistical metrics, the R^2 values for SEBS are actually comparable to those of PT-JPL
536 and GLEAM, or even higher for a majority of towers that have an aridity index less than 0.7.
537 Inspection of individual tower-based scatterplots for each of the models (not shown) illustrated
538 that while the SEBS evaporation has a strong linear relationship with observed values for a
539 majority of towers, the linear regression line exhibits a large slope, indicating an overestimation
540 in SEBS predictions. Those towers that exhibit drops in NSE (and rise in RE) for the SEBS model
541 (e.g. DE-Tha, NL-Loo, US-Wrc, FR-Pue; see [Table A1](#)) are located mainly in shrubland and forest
542 biomes, suggesting a dependency of SEBS model performance that is tied to land surface
543 vegetation characteristics. Although statistical variations are evident in all models, the greater
544 response variability in SEBS is likely due to problems in simulating heat transfer within the
545 roughness sub-layer (RSL), which often forms over tall and heterogonous land surfaces
546 (Harman, 2012). We explore the issue of skill dependency of certain models to biome type and
547 climate zone in Sections 3.2 and 3.3.

548 As noted, Figure 4 shows a general decrease in the predictive skill in all models where towers
549 have an aridity index less than 0.7, but particularly so for PM-Mu and SEBS. These reductions
550 may in part be due to data uncertainties in tower observations that originate from the
551 advection of dry air into the tower footprint, or to a reduced capacity of the models to
552 reproduce the evaporative response when evaporation represents a small fraction of the total
553 available energy. Two towers at which all models display poor performance are IT-Noe and IL-
554 Yat (see Figure 1). It seems likely that IT-Noe is influenced by strong advection of moist air from
555 the Mediterranean Sea, while IL-Yat is influenced by advection of hot and dry air from

Matthew McCabe 13/12/2015 4:09 PM

Deleted: Table A1

surrounding desert regions. None of the models in this study are able to specifically account for advection and are thus prone to misrepresenting the observed evaporative response.

3.2 Performance of the models across biomes

The variability in model performance across the tower sites observed in Figure 4 and Figure A2, indicates that a biome-specific assessment could be useful to determine whether the performance of the models is also correlated to the underlying land cover, in addition to any aridity influence. Figure 5 presents the R^2 , RE and NSE for each of the models for the seven different biome classes. The analysis was conducted using the higher quality tower-based simulations for all available 3-hourly data. One immediate highlight from Figure 5 is the relatively poor performance of all models over shrubland sites, where low values of NSE (i.e. $NSE \leq 0.05$) and reduced R^2 can be observed. Ershadi et al. (2014) observed a similarly poor response over shrublands in a separate tower-based analysis that employed some of the same models examined here. They attributed the result to difficulties in the parameterization of the models over such landscapes due to the strong heterogeneities present in these environments, as well as inherent water limitations. For instance, the capacity of the GIMMS NDVI data with 8 km spatial resolution is clearly insufficient in effectively parameterizing the roughness for SEBS, resistances for PM-Mu and constraint functions for the PT-JPL.

Excluding shrublands from the analysis, the PT-JPL is one of the best performing models across the remaining biomes, having the highest values of NSE and R^2 and lowest relative errors. Consistency in the performance of PT-JPL across biome types has been reported in earlier studies (Vinukollu et al., 2011a; Ershadi et al., 2014) and was variously ascribed to the formulation of its constraint functions (see Section 2.2.2) and the minimal forcing data requirements, which reduce its sensitivity to uncertainties in input data. GLEAM closely follows PT-JPL for evergreen needleleaf forest and grassland biomes, but shows marginally lower NSE values for other biomes. Figure 5 also indicates that while SEBS has relatively high values of R^2 over the majority of biome types, it fails to provide sufficient predictive skill for the estimation of evaporation over shrublands and forest biomes. These biome types are characterized by tall and heterogeneous canopies, within which the roughness sub-layer forms. The reduced

585 capacity of the SEBS flux gradient functions in simulating heat transfer within the roughness
586 sub-layer has been highlighted previously (Weligepolage et al., 2012; Ershadi et al., 2014).
587 Although performing poorly in shrubland and forest biomes, the SEBS model exhibits a
588 comparatively good performance across wetlands, grasslands and croplands, where shorter
589 canopies dominate. PM-Mu presents the lowest values of R^2 across all biomes, although the
590 model presents reasonable NSE values over cropland (0.64) and broadleaf forest (>0.54)
591 biomes. Improved performance of the PM-Mu model over croplands has been observed in a
592 recent study (Ershadi et al., 2015), but the key reasons for low R^2 values of the model across
593 other biomes is not immediately apparent and requires further investigation.

594 Percentile plots of the 3-hourly tower-based results were used to identify whether a model
595 under- or over-estimates evaporation across its distribution function. From Figure 6 it can be
596 seen that SEBS clearly overestimates while PM-Mu underestimates evaporation across all
597 biome types, reflecting those results presented in Figure 2. The percentile plots for SEBS are
598 close to the 1:1 line for grassland and cropland biomes that have short canopy height,
599 confirming the observations made for Figure 4 and Figure 5. PT-JPL shows good model
600 reproduction of observed values over grassland and deciduous broadleaf forest biomes, with
601 the percentile plots close to the 1:1 line. However, the model slightly underestimated
602 evaporation for croplands and overestimated evaporation for wetlands, with the tails
603 (percentiles greater than Q_{75}) reflecting greater divergence than the bulk of the distribution.
604 The rate of overestimation was higher for evergreen needleleaf forest, evergreen broadleaf
605 forest and for shrubland biomes. Figure 6 also shows that GLEAM presents strong performance
606 over grasslands, croplands and evergreen needleleaf forest sites, underestimated evaporation
607 across deciduous broadleaf forest sites and tended to overestimate evaporation across the
608 remaining biomes (wetlands, shrublands and evergreen broadleaf forests).

609 Overall, all models show a tendency towards reduced performance when applied over forest
610 biomes, but improved performance over shorter canopies. These results may be reflecting the
611 fundamental physical basis behind approaches such as the base Penman-Monteith (Penman,
612 1948), Priestley-Taylor (Priestley and Taylor, 1972) and Monin-Obukhov flux gradient functions,

Matthew McCabe 13/12/2015 2:56 PM

Deleted: but

Matthew McCabe 13/12/2015 2:54 PM

Deleted: and

615 which were developed for such surface types (Brutsaert, 1982), highlighting the challenges
616 inherent in global scale application of such models, especially over diverse land cover types.

617 To further evaluate the influence of biome type on evaporation estimation and to discriminate
618 the role of individual forcing variables in impacting model efficiencies, the *NSE* and R^2 values
619 between tower- and grid-based data were calculated for the flux response, as well as for key
620 forcing variables such as net radiation, land surface temperature, air temperature, wind speed,
621 specific humidity, fractional vegetation cover and leaf area index. As can be seen in Figure 7,
622 agreement between tower-based and grid-based net radiation data is relatively high across all
623 biomes, but especially so over forest biomes ($NSE \geq 0.67$). Grid-based wind speed data have the
624 most variable agreement with tower data, with R^2 and *NSE* values generally lower than other
625 selected variables across all of the examined biomes. Air temperature shows good agreement,
626 with both high *NSE* values ($NSE \geq 0.7$) and high R^2 values ($R^2 \geq 0.84$). Specific humidity data are
627 also well reproduced ($NSE \geq 0.72$), as is land surface temperature with an $NSE \geq 0.80$ for all
628 biomes. In sharing a common GIMMS-NDVI based derivation, the agreement for fractional
629 vegetation cover and leaf area index data is reasonable over the majority of biomes, except
630 over evergreen broadleaf forest, where both the R^2 and *NSE* are low.

631 The lower panel of Figure 7 show R^2 and *NSE* values for both the tower- and grid-based
632 simulations against eddy-covariance observations for each of the models, discriminated by
633 biome type. As can be seen, the performance of all models is reduced across all biomes when
634 grid-based forcing data is used, a result reflected in all cases by relatively lower *NSE* and R^2
635 values. PM-Mu had the smallest and SEBS had the largest decrease in performance over a
636 majority of the biomes, in accordance with the findings of Section 3.1. PT-JPL and PM-Mu had a
637 relatively constant decrease in *NSE* and R^2 for the grid-based simulations. Decreased modelling
638 performance was also maintained for GLEAM, except over the single evergreen broadleaf forest
639 tower, where a more significant departure (relative to the other biome types), was observed.
640 SEBS showed a much larger variability in performance reduction, with smaller variations due to
641 forcing over forest biomes and larger reductions over biomes with shorter canopies. The
642 significant decrease in *NSE* for SEBS over grassland, cropland and to some extent the wetland
643 biome, cannot be immediately associated with *NSE* or R^2 changes in any of the forcing variables.

644 It is interesting that the agreement over grassland and cropland biomes between tower- and
645 grid-based variables is amongst the highest (especially for wind speed, fractional vegetation
646 cover and for leaf area index data), yet the subsequent model performance is among the worst.
647 The use of global statistics to evaluate model response makes discriminating the cause of this
648 variability difficult. It is possible that the statistics are biased low due to the influence of one or
649 a few individual towers, by errors in the forcing fields driving model parameterizations (i.e.
650 vegetation height) or in response to model sensitivities to particular forcing variables. Either
651 way, these results highlight the difficulties in diagnosing the cause of performance response
652 and related sensitivity to forcing data variables in complex process-based models, which often
653 display a high degree of interactions between the variables. Indeed, diagnosing the forcing
654 variables responsible for reducing the efficiency of particular models is not feasible with a
655 simple correlation analysis of the input data fields, but requires a separate and focused
656 sensitivity analysis.

657 **3.3 Performance of the Models over Climate Zones**

658 Similar to the biome-wise analyses, an evaluation of the models was conducted across a
659 number of distinct climate zones, with R^2 , RE and NSE values for tower-based 3-hourly
660 evaporation estimations shown in Figure 8. Yet again, the results highlight the importance of
661 considering a range of evaluation metrics, as the models display some variability relative to the
662 statistical measure being employed. Overall, both PT-JPL and GLEAM maintain a consistently
663 good performance over the majority of climate zones, with PT-JPL expressing a slightly
664 improved response over all zones except temperate, where GLEAM shows an improved
665 simulation. In terms of R^2 , PM-Mu presents the lowest values overall, while SEBS exhibits high
666 values over the majority of climate zones, similar to the biome based analysis. However, SEBS
667 generally fails to reproduce the observed evaporation response, with high RE and low NSE . All
668 models have their best performance over the temperate-continental climate zone, with high
669 NSE and R^2 and low RE , which was followed closely by the temperate climate zone. The lowest
670 overall performance for all models corresponded to the dry climate zone, again reflecting the
671 aridity based results in Figure 4. As discussed in Section 3.1, data uncertainties due to the role

of advection in dry regions and difficulties in the accurate estimation when confronted with low evaporative fractions are likely reasons behind such performance reductions in dry regions.

Figure 9 displays the corresponding percentile plots of model performance over the five different climate zones. As can be seen, PT-JPL and GLEAM provide generally good performance over all climate zones, although GLEAM slightly underestimates evaporation for temperate-continental and boreal climate zones. SEBS overestimates relative to tower-based evaporation across all biomes, while PM-Mu generally underestimates, except over temperate and temperate-continental climate zones, for which the percentile plot of PM-Mu are relatively close to the 1:1 line.

Similar to Figure 7, Figure 10 outlines the model response differentiated for the different climate zones when using grid-based forcing data. As can be seen from the lower panel, the simulation performance is reduced across all climate zones, relative to the tower data. In particular, SEBS is significantly impacted across the majority of climate zones, with both a reduction in NSE and R^2 , except over boreal forests. One possible reason for this smaller variation over boreal forests could be due to lower surface-to-air temperature gradients over forests, which contributes to smaller sensible heat fluxes and consequently larger evaporative fraction values (in contrast to model performance over dry climates, where the temperature gradient is large). Nevertheless, the relationship between uncertainty in individual variables and the reduction of modelling performances is not able to be determined here. Further analysis examining the sensitivity of individual models to their forcing is required.

4 Discussion

Understanding the role of model forcing in influencing simulation results, as well as examining the impacts of biome type and climate zone on flux response, are important elements in the development of robust globally-distributed evaporation products. The focus of this study was on evaluating a set of process-based models, to support the development of globally distributed and long term observations of surface fluxes as part of the GEWEX LandFlux project. Overall, the PT-JPL and GLEAM models provided the most consistent performance, while PM-

700 Mu tended to underestimate and SEBS overestimate evaporation relative to the forty-five eddy-
701 covariance tower observations examined here. However, while statistical analysis allows a
702 pseudo-ranking of model performance, more detailed evaluation across towers, and biome and
703 climate types highlighted the considerable within-model variability in performance. Results also
704 demonstrated that changing the scale of input forcing data from tower- to grid-based reduced
705 the quality of model estimates in all cases, but especially for SEBS, where a sensitivity to
706 surface-air temperature gradients plays a strong role. In the following, we examine these
707 results and interpret any implications for large-scale global applications.

708 With its relatively simple modelling structure, PT-JPL performed consistently well relative to the
709 other models that have more complex structures and parameterization configurations. One
710 possible reason for this response may relate to the constraint functions of PT-JPL serving a wide
711 range of hydro-meteorological conditions, encompassing energy-limited (e.g. boreal climate) to
712 water-limited (e.g. dry climate) conditions. The good performance of PT-JPL was also observed
713 in a recent multi-model evaluation study, with a summary of the strengths and limitations of
714 the model presented in Ershadi et al. (2014). GLEAM also performed well, both at the tower
715 and at the grid-scale (see Figure 4 and Figure A2). Previous studies have shown that the model
716 is sensitive to the accuracy of precipitation data (Miralles et al., 2011b), as this determines the
717 partitioning of intercepted evaporation in the model and the root-zone soil moisture.
718 Unfortunately, testing for such sensitivities was not possible here, as both tower- and grid-
719 based records were filtered for rainfall events in post-processing steps, in response to the
720 limitation of eddy-covariance observations during such events.

721 In terms of the NSE , R^2 and RE , PM-Mu followed PT-JPL and GLEAM, with the model tending to
722 underestimate evaporation when applied to most of the tower- and grid-based records. While
723 reasons for this underestimation are not immediately clear, a recent study examining the
724 structure and parameterization of Penman-Monteith type models (Ershadi et al., 2015) showed
725 that the PM-Mu, which has a three-source structure, underperformed relative to a single-
726 source (Monteith, 1965) and a two-layer approach (Shuttleworth and Wallace, 1985) across all
727 studied biome types, except croplands. An interesting aspect of Ershadi et al. (2015) was that
728 application of the canopy transpiration resistance scheme of the PM-Mu in those simpler

Matthew McCabe 13/12/2015 3:10 PM

Deleted:

Matthew McCabe 13/12/2015 3:10 PM

Deleted: ,

731 models improved their prediction skills. As such, the reduced performance of the PM-Mu
732 predictions might relate to underlying structural and parameterization issues in the model. As
733 the operational model behind the generation of the current MOD16 global evaporation product
734 (Mu et al., 2013), further studies to diagnose the cause of these responses are required.

735 Regarding assessment against the tower-based eddy-covariance observations, SEBS performed
736 relatively poorly in most statistical metrics when compared to the other models, as it
737 overestimated evaporation across a majority of studied biomes and climate zones, except over
738 grasslands and cropland sites with short canopies (e.g. less than 3 m). Interestingly, even
739 though generally over-predicting results, it had one of the highest R^2 values, indicating good
740 correlation with the eddy-covariance observations. Findings from Ershadi et al. (2014) confirm
741 the good performance of the model over short canopies and its lack of performance over
742 shrublands and forests. In terms of performance against underlying biome type, it was
743 observed that any performance reduction was observed mainly across shrublands and forest
744 biomes, where the roughness sub-layer forms above the canopy (Harman, 2012). Importantly,
745 the flux-gradient functions of the SEBS model are not parameterized to effectively simulate the
746 heat transfer process in the roughness sub-layer, and hence the model fails to perform well
747 (Weligepolage et al., 2012). The reliance of SEBS on an accurate representation of the surface-
748 air temperature gradient also limits the effectiveness of the model for global application,
749 demanding improvements in characterizing the spatial and temporal representativeness of such
750 variables.

751 It is apparent from Sections 3.2 and 3.3 that the application of gridded data for modelling
752 evaporation inevitably reduces the predictive performance of all models, regardless of their
753 complexity in the evaporation process or their economy in forcing data requirements. In fact,
754 the footprint mismatch between the tower- and grid-based simulations is likely to increase
755 uncertainties in the forcing data and cause discrepancies between the simulated and tower-
756 based evaporation values. Importantly, comparing the models for their relative performance
757 (see Figure 7 and Figure 10) reveals that the performance decrease for grid-based analysis was
758 not equal amongst all of the models. For instance, SEBS was observed to be more sensitive to
759 the use of gridded forcing data, most likely as a result of inconsistencies in temperature

Matthew McCabe 10/12/2015 4:37 PM

Formatted: Left

Matthew McCabe 13/12/2015 3:14 PM

Deleted: In terms of

761 gradient fields: an aspect that has been noted previously (van der Kwast et al., 2009; Ershadi et
762 al., 2013). Although input uncertainty also impacts the performance of PT-JPL, PM-Mu and
763 GLEAM, the *NSE* and R^2 of gridded simulations for those models are closer to their tower-based
764 counterparts. Apart from indicating a robust model structure, the reduced impact seen in these
765 schemes may also be a consequence of avoiding the use of forcing data such as land surface
766 temperature and wind speed data, which are known to be uncertain at both the grid and
767 tower-scale. Regardless of the culprit behind the observed performance discrepancy between
768 tower and grid-based simulations, it is clear that some models are better suited to global
769 application than others – at least given the quality of currently available global forcing datasets.

770 Importantly, the results presented in Sections 3.2 and 3.3 showed that evaluating tower or grid-
771 based statistical responses alone is not enough to identify those forcing variables most
772 impacting model performance. Diagnosing forcing sensitivity is not trivial given non-linearities
773 in the models and the high level of interaction within model variables and parameters. Indeed,
774 caution is warranted in any approaches seeking to evaluate evaporation models using gridded
775 data in isolation, as this is likely to yield unreliable performance metrics of the models. It is
776 important to perform a parallel tower-based data assessment to increase confidence in any
777 single models performance (Su et al., 2005) in any evaluation approach, particularly those
778 occurring at global scales.

779 Although the largest possible set of eddy-covariance towers and a common set of forcing data
780 was used to evaluate the different model simulations, there are still inevitable limitations in the
781 evaluations. Identifying such limitations is important not only for the current evaluations, but
782 also in guiding future contributions. One such example relates to the period of tower data used
783 for evaluation in this study (see Figure A1), as the data record length varies amongst the towers
784 and the data are not uniformly distributed across seasons. Moreover, the towers are not evenly
785 distributed across the studied biomes and climate zones (see Figure 1, Table A1), with only one
786 tower covering the entire evergreen broadleaf forest biome and two towers covering the
787 wetland biome. Further, no towers were available for use in arctic and tropical climate zones.
788 Although the tropical climate zone, especially Amazonian forests, is accounted as a critical
789 component in studies of the global water and energy cycles (Chahine, 1992; Wohl et al., 2012),

Matthew McCabe 13/12/2015 3:15 PM
Deleted: ,

Matthew McCabe 13/12/2015 4:09 PM
Deleted: Figure A1

Matthew McCabe 13/12/2015 4:09 PM
Deleted: Table A1

793 relatively few towers in this zone provide land surface temperature and longwave upward
794 radiation data needed for the SEBS model. An additional limitation is the coarse (8 km) spatial
795 resolution of the GIMMS NDVI data used in the models for the tower-based analysis, as this
796 resolution certainly does not correspond with the footprint of eddy-covariance sensors at any
797 of the towers. Developments towards improving the availability and access to long-term high-
798 resolution Landsat images (e.g. via Google Earth Engine; <https://earthengine.google.org>) might
799 be one way to improve model forcing and evaluation exercises, especially with the
800 development of high-resolution vegetation products ([Houborg et al. 2016](#)).

801 While the accuracy of individual variables in the LandFlux dataset were enhanced by bias
802 correction against independent data sources (see Section 2.1), diagnosing the internal
803 consistency of the data fields (McCabe et al., 2008), especially for air temperature, land surface
804 temperature, wind speed and humidity, is a concept that has not received much attention to
805 date and demands more considered investigations and analysis. Internal consistency is an
806 extremely challenging objective, but is critically important for flux estimation, where so many
807 different forcing data are required. Essentially it demands that all required model data are
808 derived from a common set of forcing variables, rather than by the standard approach of
809 compilation based on availability and accessibility. The most illustrative example would be in
810 the development of radiation data, derived here from NASA-GEWEX SRB sources (Stackhouse et
811 al., 2011). Calculation of radiation components requires air temperature, surface temperature,
812 land surface and vegetation features, as well as numerous other elements. However, these
813 underlying variables are rarely if ever retained to provide a consistent overall forcing data set
814 (i.e. the meteorological variables used in producing the SRB data are not subsequently used to
815 drive the models). Interdependencies in forcing affect many variables in the estimation of
816 evaporation, yet products are not developed with this simple consistency principle in mind.
817 Apart from introducing further biases and uncertainties into model simulations, until such
818 consistency is attained, discriminating between the impact of forcing versus the model
819 sensitivity to that forcing will remain extremely challenging.

820 From one perspective, the performance of the evaporation models examined here seems
821 relatively poor, even when they are forced with high-quality tower-based data. PT-JPL, which

Matthew McCabe 13/12/2015 3:19 PM

Deleted: (Houborg et al., 2015)

823 was identified as one of the most consistent and best performing models, still presented a
824 relative error of 41%, with errors for GLEAM, PM-Mu and SEBS of 43%, 52% and 72%,
825 respectively. However, it is important to recognise that tower-based evaluation represents one
826 of the strictest measure of model performance and comes with its own caveats. One question
827 that remains unanswered is whether it is even appropriate to expect models run with large-
828 scale gridded forcing to replicate the small-scale response observed by eddy-covariance towers.
829 The alternative perspective, given inherent uncertainties in forcing, observations and
830 specification of model parameters, is that these results are encouraging. Broader scale metrics
831 such as hydrological consistency (McCabe et al., 2008), catchment based assessments or water
832 budget closure approaches would provide a better guide (Sheffield et al., 2009) and indeed,
833 such evaluations will need to be performed. These questions highlight the difficulties in not just
834 producing global estimates, but perhaps more importantly, in evaluating their quality.

835 The observed variability of modelling performance across the studied biomes and climate zones
836 implies that caution is required in advocating any single model for large-scale or global
837 application. These results reflect previous findings that any one modelling approach is
838 incapable of accurately reflecting the range of flux responses occurring across diverse
839 landscapes (Ershadi et al., 2014; Ershadi et al., 2015). One possible solution to address this
840 inherent model limitation is to assemble a mosaicked product based on the predictive skill of
841 the model(s) over particular biomes or climate zones. Another approach might be to develop an
842 ensemble product using a suitable multi-model blending technique, such as a Bayesian Model
843 Averaging approach (Hoeting et al., 1999; Yao et al., 2014). Either way, it is clear that further
844 multi-model assessments are required for progressing global scale flux characterisation and to
845 ensure a robust and representative product is developed.

846

847 5 Conclusions

848 It is something of a contradiction that the global-scale estimation of surface fluxes is both
849 straightforward and extremely challenging at the same time. It is more straightforward than
850 ever due to the availability of needed forcing data from various sources, such as numerical

Matthew McCabe 10/12/2015 11:18 AM
Deleted: is perhaps

Matthew McCabe 10/12/2015 11:18 AM
Deleted:

Matthew McCabe 13/12/2015 3:22 PM
Deleted: outstanding

Matthew McCabe 10/12/2015 11:20 AM
Deleted: Perhaps b

855 weather prediction or other operational products, as well as the increased development of
856 global satellite based datasets. However, the comparative ease with which products can be
857 developed belies the difficulties in actually developing robust and coherent simulations.
858 Uncertainties in the use of internally inconsistent forcing data, the influence of untested model
859 parameterizations over different land surface and climate types, violation of model
860 assumptions in their graduation from the local scale to global scale and the perennial question
861 on how to best evaluate model output all seek to confound global flux efforts.

862 The evaluation of four process-based evaporation models as part of the GEWEX LandFlux
863 | project, undertaken here over a range of biome types and climate zones, highlighted the
864 variable performance and verified the sentiment that no single model is able to consistently
865 outperform any other. While individual model results at the tower scale allowed for a relative
866 performance ranking, the overall model errors when considered globally were high. Of those
867 | models assessed here and being considered as potential candidates for a GEWEX LandFlux
868 product, PT-JPL and GLEAM represent the most likely schemes for providing consistent
869 simulation response over a range of biome and climate types. In a challenge for the
870 development of more accurate global flux products, application of gridded data reduces the
871 performance of all models, even if the overall performance ranking does not change between
872 simulation runs. Such a response has obvious implications when model simulations at the
873 continental and global scales are increasingly required in many applications and where not only
874 the forcing data have large uncertainties, but also the underlying assumptions of the models
875 themselves are likely to be questioned. Further investigations on the reasons for such variable
876 performance and ways to offset the inherent uncertainties in global forcing are required.
877 Additional research is also needed to improve the structure and parameterization of some of
878 | these candidate models, to understand model sensitivities to forcing (by conducting a thorough
879 sensitivity analysis) and to develop and implement an appropriate ensemble modelling and
880 merging technique that takes advantage of individual model performance over defined regions.
881 Further detailed comparisons against estimates from more complex modelling systems, such as
882 | reanalysis and numerical weather prediction models, are needed to provide greater context
883 and additional benchmarking metrics to guide future investigations.

Matthew McCabe 13/12/2015 3:24 PM

Deleted: ,

Matthew McCabe 13/12/2015 3:25 PM

Deleted: -

Matthew McCabe 13/12/2015 3:28 PM

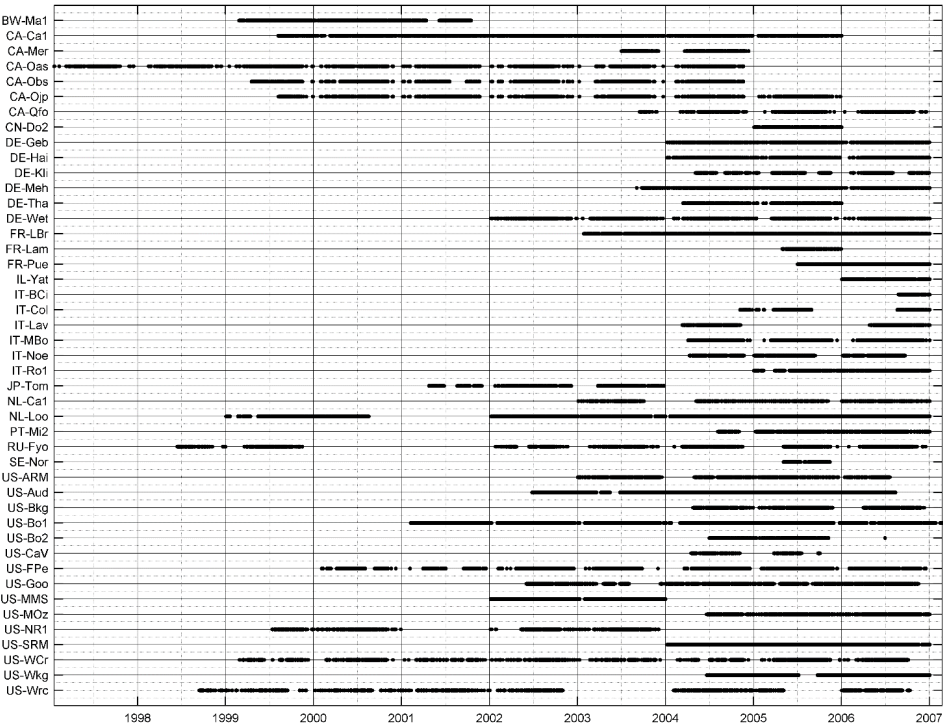
Deleted: also necessary tasks for

888 **Appendix A: Description of Tower Locations**

889 Table A1: Selected eddy-covariance and their attributes. [Further details and information on](#)
890 [individual tower sites can be found via the Fluxnet data portal \(<http://fluxnet.fluxdata.org/>\)](#)

Site-ID	Country	Lat.	Lon.	Ground Elev. (masl)	Tower height (m)	IGBP	Climate Class	
BW-Ma1	Botswana	-19.9	23.6	947	12.6	WSA	BSh	
CA-Ca1	Canada	49.9	-125.3	324	43	ENF	Cfb	
CA-Mer	Canada	45.4	-75.5	68	3	WET	Dfb	
CA-Oas	Canada	53.6	-106.2	594	39	DBF	Dfc	
CA-Obs	Canada	54.0	-105.1	593	25	ENF	Dfc	
CA-Ojp	Canada	53.9	-104.7	517	28	ENF	Dfc	
CA-Qfo	Canada	49.7	-74.3	389	25	ENF	Dfc	
CN-Do2	China	31.6	121.9	4	5	WET	Cfa	
DE-Geb	Germany	51.1	10.9	159	6	CRO	Cfb	
DE-Hai	Germany	51.1	10.5	458	43.5	DBF	Cfb	
DE-Kli	Germany	50.9	13.5	480	3.5	CRO	Cfb	
DE-Meh	Germany	51.3	10.7	289	3	GRA	Cfb	
DE-Tha	Germany	51.0	13.6	387	42	ENF	Cfb	
DE-Wet	Germany	50.5	11.5	789	27	ENF	Cfb	
FR-LBr	France	44.7	-0.8	71	41	ENF	Cfb	
FR-Lam	France	43.5	1.2	182	3.65	CRO	Cfb	
FR-Pue	France	43.7	3.6	271	13	EBF	Csa	
IL-Yat	Israel	31.3	35.1	654	18	ENF	BSh	
IT-BCi	Italy	40.5	15.0	9	2	CRO	Csa	
IT-Col	Italy	41.8	13.6	1534	25	DBF	Cfa	
IT-Lav	Italy	46.0	11.3	1367	33	ENF	Cfb	
IT-MBo	Italy	46.0	11.0	1563	2.5	GRA	Cfb	

Site-ID	Country	Lat.	Lon.	Ground Elev. (masl)	Tower height (m)	IGBP	Climate Class	Climate
								Matthew McCabe 13/12/2015 3:41 PM Formatted: Space Before: 0 pt
IT-Noe	Italy	40.6	8.2	27	<u>3.6</u>	CSH	Csa	Matthew McCabe 13/12/2015 3:41 PM Formatted: None, Space Before: 0 pt, No bullets or numbering, Don't keep with next, Don't keep lines together
IT-Ro1	Italy	42.4	11.9	174	<u>20</u>	DBF	Csa	Matthew McCabe 13/12/2015 3:41 PM Formatted: None, Space Before: 0 pt, No bullets or numbering, Don't keep with next, Don't keep lines together
JP-Tom	Japan	42.7	141.5	133	<u>42</u>	MF	Dfb	Matthew McCabe 13/12/2015 3:41 PM Formatted: None, Space Before: 0 pt, No bullets or numbering, Don't keep with next, Don't keep lines together
NL-Ca1	Netherlands	52.0	4.9	-1	<u>5</u>	GRA	Cfb	Matthew McCabe 13/12/2015 3:41 PM Formatted Table
NL-Loo	Netherlands	52.2	5.7	34	<u>27</u>	ENF	Cfb	Matthew McCabe 13/12/2015 3:41 PM Formatted Table
PT-Mi2	Portugal	38.5	-8.0	191	<u>2.5</u>	GRA	Csa	Matthew McCabe 13/12/2015 3:41 PM Formatted Table
RU-Fyo	Russia	56.5	32.9	274	<u>29</u>	ENF	Dfb	Matthew McCabe 13/12/2015 3:41 PM Formatted Table
SE-Nor	Sweden	60.1	17.5	35	<u>103</u>	ENF	Dfb	Matthew McCabe 13/12/2015 3:41 PM Formatted Table
US-ARM	USA	36.6	-97.5	318	<u>60</u>	CRO	Cfa	Matthew McCabe 13/12/2015 3:41 PM Formatted Table
US-Aud	USA	31.6	-110.5	1474	<u>4</u>	GRA	BSk	Matthew McCabe 13/12/2015 3:41 PM Formatted Table
US-Bkg	USA	44.3	-96.8	496	<u>4</u>	GRA	Dfa	Matthew McCabe 13/12/2015 3:41 PM Formatted Table
US-Bo1	USA	40.0	-88.3	218	<u>10</u>	CRO	Dfa	Matthew McCabe 13/12/2015 3:41 PM Formatted Table
US-Bo2	USA	40.0	-88.3	220	<u>10</u>	CRO	Dfa	Matthew McCabe 13/12/2015 3:41 PM Formatted Table
US-CaV	USA	39.1	-79.4	993	<u>4</u>	GRA	Cfb	Matthew McCabe 13/12/2015 3:41 PM Formatted Table
US-FPe	USA	48.3	-105.1	632	<u>3.5</u>	GRA	BSk	Matthew McCabe 13/12/2015 3:41 PM Formatted Table
US-Goo	USA	34.3	-89.9	94	<u>4</u>	GRA	Cfa	Matthew McCabe 13/12/2015 3:41 PM Formatted Table
US-MMS	USA	39.3	-86.4	290	<u>48</u>	DBF	Cfa	Matthew McCabe 13/12/2015 3:41 PM Formatted Table
US-MOz	USA	38.7	-92.2	238	<u>30</u>	DBF	Cfa	Matthew McCabe 13/12/2015 3:41 PM Formatted Table
US-NR1	USA	40.0	-105.5	3053	<u>26</u>	ENF	Dfc	Matthew McCabe 13/12/2015 3:41 PM Formatted Table
US-SRM	USA	31.8	-110.9	1120	<u>6.4</u>	WSA	BSk	Matthew McCabe 13/12/2015 3:41 PM Formatted Table
US-WCr	USA	45.8	-90.1	524	<u>30</u>	DBF	Dfb	Matthew McCabe 13/12/2015 3:41 PM Formatted Table
US-Wkg	USA	31.7	-109.9	1522	<u>6.4</u>	GRA	BSk	Matthew McCabe 13/12/2015 3:41 PM Formatted Table
US-Wrc	USA	45.8	-122.0	391	<u>85</u>	ENF	Csb	Matthew McCabe 13/12/2015 3:41 PM Formatted Table



893

894

895

896

897

Figure A1: Temporal duration of the eddy-covariance based flux and tower meteorological observations for each of the 45 sites used in this study

Matthew McCabe 13/12/2015 3:43 PM

Deleted: Period

Matthew McCabe 13/12/2015 3:43 PM

Deleted: for

Matthew McCabe 13/12/2015 3:43 PM

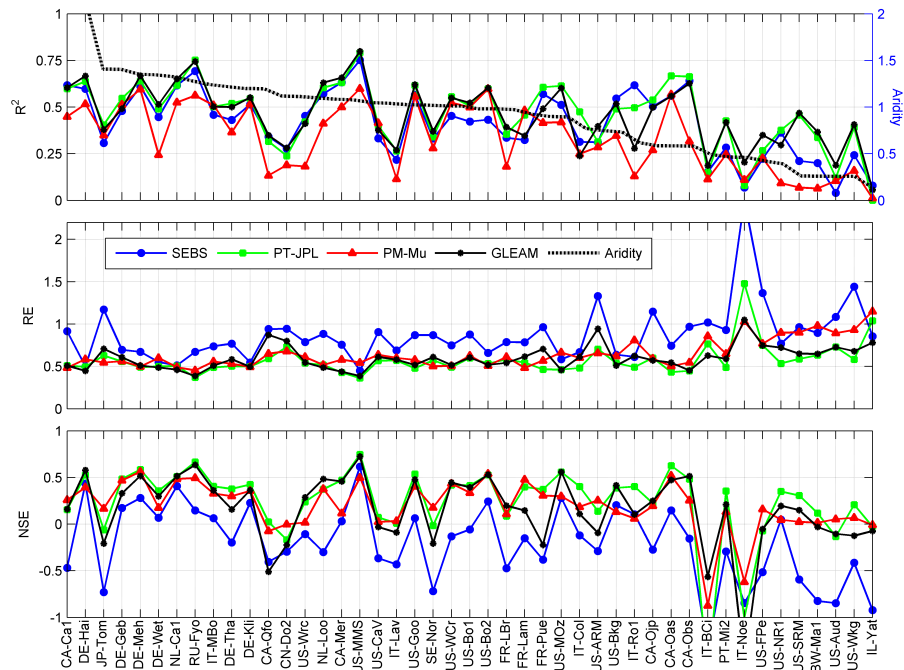
Deleted: available

Matthew McCabe 13/12/2015 3:44 PM

Deleted: records

Matthew McCabe 13/12/2015 3:43 PM

Deleted: for the towers that were used in this study



Unknown
Formatted: Font: +Theme Body, 12 pt, Bold, Font color: Auto

Figure A2: Comparison of the performance skill of the models in reproducing evaporation for the grid-based analyses. R^2 is the coefficient of determination, RE is relative error (lower is better) and NSE is the Nash-Sutcliffe Efficiency (higher is better). Towers are arranged from left to right based on aridity index.

910 **Code Availability**

911 The PM-Mu, SEBS and PT-JPL models were coded in MATLAB as part of the GEWEX LandFlux and
912 WACMOS-ET projects, in discussion with (but independent of) the principal model authors, as
913 referenced in the relevant publications. The GLEAM model was developed in MATLAB by Diego Miralles
914 and Brecht Martens. All model code can be made available upon an emailed request to
915 hydrology@kaust.edu.sa, including a brief description of the intended purpose and application.

916 **Data Availability**

917 Evaporation model output presented here for both the gridded and tower based analyses can be
918 provided upon an emailed request to hydrology@kaust.edu.sa. The request should include a brief
919 description of the intended purpose and application of the model data.

920 **Acknowledgements**

921 Research reported in this publication was supported by the King Abdullah University of Science
922 and Technology (KAUST). D.G.M. acknowledges the financial support from The Netherlands
923 Organization for Scientific Research through grant 863.14.004. We appreciate the support of
924 the ESA funded WACMOS-ET project for both fruitful scientific discussions and guidance in
925 ensuring complementarity of these joint efforts. We thank the FLUXNET site investigators for
926 allowing the use of their meteorological data. This work used eddy-covariance data acquired by
927 the FLUXNET community and in particular by the AmeriFlux program (U.S. Department of
928 Energy, Biological and Environmental Research, Terrestrial Carbon Program: DE-FG02-
929 04ER63917 and DE-FG02-04ER63911), AfriFlux, AsiaFlux, CarboAfrica, CarboEuropeIP,
930 CarboItaly, CarboMont, ChinaFlux, Fluxnet-Canada (supported by CFCAS, NSERC, BIOCAP,
931 Environment Canada, and NRCan), GreenGrass, KoFlux, LBA, NECC, TCOS-Siberia, USCCC. We
932 acknowledge the financial support to the eddy-covariance data harmonization provided by
933 CarboEuropeIP, FAO-GTOS-TCO, iLEAPS, Max Planck Institute for Biogeochemistry, National
934 Science Foundation, University of Tuscia, Université Laval and Environment Canada and US
935 Department of Energy and the database development and technical support from Berkeley
936 Water Centre, Lawrence Berkeley National Laboratory, Microsoft Research eScience, Oak Ridge
937 National Laboratory, University of California - Berkeley, University of Virginia.

938

939 **References**

- 940 Adler, R. F., Huffman, G. J., Chang, A., Ferraro, R., Xie, P. P., Janowiak, J., Rudolf, B., Schneider, U., Curtis,
 941 S., Bolvin, D., Gruber, A., Susskind, J., Arkin, P., and Nelkin, E.: The version-2 global precipitation
 942 climatology project (GPCP) monthly precipitation analysis (1979-present), Journal of
 943 Hydrometeorology, 4, 1147-1167, 2003.
- 944 Allen, R. G.: Using the FAO-56 dual crop coefficient method over an irrigated region as part of an
 945 evapotranspiration intercomparison study, Journal of Hydrology, 229, 27-41, 2000.
- 946 Allen, R. G., Tasumi, M., and Trezza, R.: Satellite-Based Energy Balance for Mapping Evapotranspiration
 947 with Internalized Calibration (METRIC)-Model, Journal of Irrigation and Drainage Engineering, 133,
 948 380-394, 2007.
- 949 Armstrong, R. L., Brodzik, M. J., Knowles, K., and Savoie, M.: Global monthly EASE-Grid snow water
 950 equivalent climatology, Boulder, CO: National Snow and Ice Data Center, Digital media, 2005.
 951 2005.
- 952 Badgley, G., Fisher, J. B., Jiménez, C., Tu, K. P., and Vinukollu, R.: On uncertainty in global terrestrial
 953 evapotranspiration estimates from choice of input forcing datasets, Journal of Hydrometeorology,
 954 doi: 10.1175/JHM-D-14-0040.1, 2015. 2015.
- 955 Baldocchi, D., Falge, E., Gu, L., Olson, R., Hollinger, D., Running, S., Anthoni, P., Bernhofer, C., Davis, K.,
 956 Evans, R., Fuentes, J., Goldstein, A., Katul, G., Law, B., Lee, X., Malhi, Y., Meyers, T., Munger, W.,
 957 Oechel, W., Paw, K. T., Pilegaard, K., Schmid, H. P., Valentini, R., Verma, S., Vesala, T., Wilson, K.,
 958 and Wofsy, S.: FLUXNET: A New Tool to Study the Temporal and Spatial Variability of Ecosystem–
 959 Scale Carbon Dioxide, Water Vapor, and Energy Flux Densities, Bulletin of the American
 960 Meteorological Society, 82, 2415-2434, 2001.
- 961 Bastiaanssen, W. G. M., Menenti, M., Feddes, R. A., and Holtslag, A. A. M.: A remote sensing surface
 962 energy balance algorithm for land (SEBAL). 1. Formulation, Journal of Hydrology, 212-213, 198-
 963 212, 1998.
- 964 Bos, M. G., Kselik, R. A. L., Allen, R. G., and Molden, D. J.: Water Requirements for Irrigation and the
 965 Environment, Springer, Dordrecht, 2008.
- 966 Bouchet, R. J.: Evapotranspiration réelle et potentielle, signification climatique. General Assembly
 967 Berkeley, International Association for Hydrological Sciences. Gentbrugge, Belgium. 62: 134-142,
 968 1963.

Matthew McCabe 13/12/2015 3:52 PM
 Formatted: Indent: Left: 0 cm, Hanging:
 1 cm

969 [Brutsaert, W.: Evaporation Into the Atmosphere : theory, history, and applications, Reidel Publishing,](#)
970 [Dordrecht etc., 1982.](#)

971 [Brutsaert, W.: Hydrology : An Introduction, Cambridge University Press, Cambridge, 2005.](#)

972 [Brutsaert, W. and Stricker, H.: An advection-aridity approach to estimate actual regional](#)
973 [evapotranspiration, Water Resour. Res., 15, 443-450, 1979.](#)

974 [Carvalhais, N., Reichstein, M., Collatz, G. J., Mahecha, M. D., Migliavacca, M., Neigh, C. S. R., Tomelleri,](#)
975 [E., Benali, A. A., Papale, D., and Seixas, J.: Deciphering the components of regional net ecosystem](#)
976 [fluxes following a bottom-up approach for the Iberian Peninsula, Biogeosciences, 7, 3707-3729,](#)
977 [2010.](#)

978 [Cavanaugh, M. L., Kurc, S. A., and Scott, R. L.: Evapotranspiration partitioning in semiarid shrubland](#)
979 [ecosystems: a two - site evaluation of soil moisture control on transpiration, Ecohydrology, 4,](#)
980 [671-681, 2011.](#)

981 [Chahine, M. T.: The hydrological cycle and its influence on climate, Nature, 359, 373-380, 1992.](#)

982 [Chen, X., Su, Z., Ma, Y., Yang, K., Wen, J., and Zhang, Y.: An Improvement of Roughness Height](#)
983 [Parameterization of the Surface Energy Balance System \(SEBS\) over the Tibetan Plateau, Journal](#)
984 [of Applied Meteorology and Climatology, 52, 607-622, 2012.](#)

985 [Chiti, T., Papale, D., Smith, P., Dalmonech, D., Matteucci, G., Yeluripati, J., Rodeghiero, M., and Valentini,](#)
986 [R.: Predicting changes in soil organic carbon in mediterranean and alpine forests during the Kyoto](#)
987 [Protocol commitment periods using the CENTURY model, Soil use and management, 26, 475-484,](#)
988 [2010.](#)

989 [Coccia, G., Siemann, A., Pan, M., and Wood, E. F.: Creating consistent datasets by combining remotely-](#)
990 [sensed data and land surface model estimates through Bayesian uncertainty post-processing: the](#)
991 [case of Land Surface Temperature from HIRS, Remote Sensing of Environment, 170, 290-305,](#)
992 [doi:10.1016/j.rse.2015.09.010, 2015.](#)

993 [Curtis, P. S., Hanson, P. J., Bolstad, P., Barford, C., Randolph, J. C., Schmid, H. P., and Wilson, K. B.:](#)
994 [Biometric and eddy-covariance based estimates of annual carbon storage in five eastern North](#)
995 [American deciduous forests, Agricultural and Forest Meteorology, 113, 3-19, 2002.](#)

996 [Delpierre, N., Soudani, K., Francois, C., Köstner, B., Pontailier, J. Y., Nikinmaa, E., Misson, L., Aubinet, M.,](#)
997 [Bernhofer, C., and Granier, A.: Exceptional carbon uptake in European forests during the warm](#)
998 [spring of 2007: a data–model analysis, Global Change Biology, 15, 1455-1474, 2009.](#)

999 [Don, A., Rebmann, C., Kolle, O., Scherer - Lorenzen, M., and Schulze, E. D.: Impact of afforestation -](#)
1000 [associated management changes on the carbon balance of grassland, Global Change Biology, 15,](#)
1001 [1990-2002, 2009.](#)

1002 [Douville, H., Ribes, A., Decharme, B., Alkama, R., and Sheffield, J.: Anthropogenic influence on](#)
1003 [multidecadal changes in reconstructed global evapotranspiration, Nature Clim. Change, 3, 59-62,](#)
1004 [2013.](#)

1005 [Dragoni, D., Schmid, H. P., Wayson, C. A., Potter, H., Grimmond, C. S. B., and Randolph, J. C.: Evidence of](#)
1006 [increased net ecosystem productivity associated with a longer vegetated season in a deciduous](#)
1007 [forest in south - central Indiana, USA, Global Change Biology, 17, 886-897, 2011.](#)

1008 [Ershadi, A., McCabe, M. F., Evans, J. P., Chaney, N. W., and Wood, E. F.: Multi-site evaluation of](#)
1009 [terrestrial evaporation models using FLUXNET data, Agricultural and Forest Meteorology, 187, 46-](#)
1010 [61, 2014.](#)

1011 [Ershadi, A., McCabe, M. F., Evans, J. P., Mariethoz, G., and Kavetski, D.: A Bayesian analysis of sensible](#)
1012 [heat flux estimation: Quantifying uncertainty in meteorological forcing to improve model](#)
1013 [prediction, Water Resources Research, 49, 2343-2358, 2013.](#)

1014 [Ershadi, A., McCabe, M. F., Evans, J. P., and Wood, E. F.: Impact of model structure and parameterization](#)
1015 [on Penman–Monteith type evaporation models, Journal of Hydrology, 525, 521-535, 2015.](#)

1016 [Famiglietti, J. S., Lo, M., Ho, S. L., Bethune, J., Anderson, K. J., Syed, T. H., Swenson, S. C., de Linage, C. R.,](#)
1017 [and Rodell, M.: Satellites measure recent rates of groundwater depletion in California's Central](#)
1018 [Valley, Geophysical Research Letters, 38\(3\), 10.1029/2010GL046442, 2011.](#)

1019 [Fisher, J. B., Tu, K. P., and Baldocchi, D. D.: Global estimates of the land-atmosphere water flux based on](#)
1020 [monthly AVHRR and ISLSCP-II data, validated at 16 FLUXNET sites, Remote Sensing of](#)
1021 [Environment, 112, 901-919, 2008.](#)

1022 [Flanagan, L. B., Cai, T., Black, T. A., Barr, A. G., McCaughey, J. H., and Margolis, H. A.: Measuring and](#)
1023 [modeling ecosystem photosynthesis and the carbon isotope composition of ecosystem-respired](#)
1024 [CO₂ in three boreal coniferous forests, Agricultural and Forest Meteorology, 153, 165-176, 2012.](#)

1025 [Fu, D., Chen, B., Zhang, H., Wang, J., Black, T. A., Amiro, B. D., Bohrer, G., Bolstad, P., Coulter, R., and](#)
1026 [Rahman, A. F.: Estimating landscape net ecosystem exchange at high spatial–temporal resolution](#)
1027 [based on Landsat data, an improved upscaling model framework, and eddy covariance flux](#)
1028 [measurements, Remote Sensing of Environment, 141, 90-104, 2014.](#)

1029 [Gamon, J. A., Coburn, C., Flanagan, L. B., Huemmrich, K. F., Kiddle, C., Sanchez-Azofeifa, G. A., Thayer, D.](#)
1030 [R., Vescovo, L., Gianelle, D., and Sims, D. A.: SpecNet revisited: bridging flux and remote sensing](#)
1031 [communities, Can. J. Remote Sens., 36, S376-S390, 2010.](#)

1032 [Gash, J. H.: An analytical model of rainfall interception by forests quarterly, Journal of Royal](#)
1033 [Meteorological Society, 105, 43-45, 1979.](#)

1034 [Gilmanov, T., Soussana, J., Aires, L., Allard, V., Ammann, C., Balzarolo, M., Barcza, Z., Bernhofer, C.,](#)
1035 [Campbell, C., Cernusca, A., Cescatti, A., Clifton-Brown, J., Dirks, B., Dore, S., Eugster, W., Fuhrer, J.,](#)
1036 [Gimeno, C., Gruenwald, T., Haszpra, L., Hensen, A., Ibrom, A., Jacobs, A., Jones, M., Lanigan, G.,](#)
1037 [Laurila, T., Lohila, A., Manca, G., Marcolla, B., Nagy, Z., Pilegaard, K., Pinter, K., Pio, C., Raschi, A.,](#)
1038 [Rogiers, N., Sanz, M., Stefani, P., Sutton, M., Tuba, Z., Valentini, R., Williams, M., and Wohlfahrt,](#)
1039 [G.: Partitioning European grassland net ecosystem CO2 exchange into gross primary productivity](#)
1040 [and ecosystem respiration using light response function analysis, Agriculture, Ecosystems and](#)
1041 [Environment, 121, 93 - 120, 2007.](#)

1042 [Gioli, B., Miglietta, F., De Martino, B., Hutjes, R. W. A., Dolman, H. A. J., Lindroth, A., Schumacher, M.,](#)
1043 [Sanz, M. J., Manca, G., and Peressotti, A.: Comparison between tower and aircraft-based eddy](#)
1044 [covariance fluxes in five European regions, Agricultural and Forest Meteorology, 127, 1-16, 2004.](#)

1045 [Göckede, M., Foken, T., Aubinet, M., Aurela, M., Banza, J., Bernhofer, C., Bonnefond, J.-M., Brunet, Y.,](#)
1046 [Carrara, A., and Clement, R.: Quality control of CarboEurope flux data–Part 1: Coupling footprint](#)
1047 [analyses with flux data quality assessment to evaluate sites in forest ecosystems, Biogeosciences,](#)
1048 [5, 433-450, 2008.](#)

1049 [Granger, R. J.: Satellite-derived estimates of evapotranspiration in the Gediz basin, Journal of Hydrology,](#)
1050 [229, 70-76, 2000.](#)

1051 [Greve, P., Orlowsky, B., Mueller, B., Sheffield, J., Reichstein, M., and Seneviratne, S. I.: Global assessment](#)
1052 [of trends in wetting and drying over land, Nature geoscience, 7, 716-721, 2014.](#)

1053 [Guillod, B. P., Orlowsky, B., Miralles, D. G., Teuling, A. J., and Seneviratne, S. I.: Reconciling spatial and](#)
1054 [temporal soil moisture effects on afternoon rainfall, Nat Commun, 6, 2015.](#)

1055 [Hansen, M. C., Townshend, J. R. G., DeFries, R. S., and Carroll, M.: Estimation of tree cover using MODIS](#)
1056 [data at global, continental and regional/local scales, Int. J. Remote Sens., 26, 4359-4380, 2005.](#)

1057 [Harman, I.: The Role of Roughness Sublayer Dynamics Within Surface Exchange Schemes, Boundary-](#)
1058 [Layer Meteorology, 142, 1-20, 2012.](#)

1059 [Hilton, T. W., Davis, K. J., and Keller, K.: Evaluating terrestrial CO₂ flux diagnoses and uncertainties from](#)
1060 [a simple land surface model and its residuals, Biogeosciences, 11, 217-235, 2014.](#)

1061 [Hirschi, M., Seneviratne, S. I., Alexandrov, V., Boberg, F., Boroneant, C., Christensen, O. B., Formayer, H.,](#)
1062 [Orlowsky, B., and Stepanek, P.: Observational evidence for soil-moisture impact on hot extremes](#)
1063 [in southeastern Europe, Nature Geoscience, 4, 17-21, 2011.](#)

1064 [Hoeting, J. A., Madigan, D., Raftery, A. E., and Volinsky, C. T.: Bayesian Model Averaging: A Tutorial,](#)
1065 [Statistical Science, 14, 382-401, 1999.](#)

1066 [Hollinger, D. Y., Ollinger, S. V., Richardson, A. D., Meyers, T. P., Dail, D. B., Martin, M. E., Scott, N. A.,](#)
1067 [Arkebauer, T. J., Baldocchi, D. D., and Clark, K. L.: Albedo estimates for land surface models and](#)
1068 [support for a new paradigm based on foliage nitrogen concentration, Global Change Biology, 16,](#)
1069 [696-710, 2010.](#)

1070 [Horn, J. E. and Schulz, K.: Identification of a general light use efficiency model for gross primary](#)
1071 [production, Biogeosciences, 8, 999 - 1021, 2011.](#)

1072 [Houborg, R., McCabe, M. F., and Gao, F.: A Spatio-Temporal Enhancement Method for medium](#)
1073 [resolution LAI \(STEM-LAI\), International Journal of Applied Earth Observation and Geoinformation,](#)
1074 [47, 15-29, 2016.](#)

1075 [Huffman, G. J., Adler, R. F., Rudolph, B., Schneider, U., and Keehn, P.: Global precipitation estimates](#)
1076 [based on a technique for combining satellite-based estimates, rain gauge analysis, and NWP](#)
1077 [model precipitation information, J. Climate, 8, 1284-1295, 1995.](#)

1078 [Humphreys, E. R., Black, T. A., Morgenstern, K., Cai, T., Drewitt, G. B., Nesic, Z., and Trofymow, J. A.:](#)
1079 [Carbon dioxide fluxes in coastal Douglas-fir stands at different stages of development after](#)
1080 [clearcut harvesting, Agricultural and Forest Meteorology, 140, 6-22, 2006.](#)

1081 [Jiménez, C., Prigent, C., Mueller, B., Seneviratne, S. I., McCabe, M. F., Wood, E. F., Rossow, W. B.,](#)
1082 [Balsamo, G., Betts, A. K., Dirmeyer, P. A., Fisher, J. B., Jung, M., Kanamitsu, M., Reichle, R. H.,](#)

1083 [Reichstein, M., Rodell, M., Sheffield, J., Tu, K., and Wang, K.: Global intercomparison of 12 land](#)
1084 [surface heat flux estimates, J. Geophys. Res., 116, D02102, 2011.](#)

1085 [Jiménez-Muñoz, J., Sobrino, J., Plaza, A., Guanter, L., Moreno, J., and Martinez, P.: Comparison Between](#)
1086 [Fractional Vegetation Cover Retrievals from Vegetation Indices and Spectral Mixture Analysis:](#)
1087 [Case Study of PROBA/CHRIS Data Over an Agricultural Area, Sensors, 9, 768-793, 2009.](#)

1088 [Jung, M., Reichstein, M., Ciais, P., Seneviratne, S. I., Sheffield, J., Goulden, M. L., Bonan, G., Cescatti, A.,](#)
1089 [Chen, J., and de Jeu, R.: Recent decline in the global land evapotranspiration trend due to limited](#)
1090 [moisture supply, Nature, 467, 951-954, 2010.](#)

1091 [Kross, A., Seaquist, J. W., Roulet, N. T., Fernandes, R., and Sonnentag, O.: Estimating carbon dioxide](#)
1092 [exchange rates at contrasting northern peatlands using MODIS satellite data, Remote Sensing of](#)
1093 [Environment, 137, 234-243, 2013.](#)

1094 [Kustas, W. P., Perry, E. M., Doraiswamy, P. C., and Moran, M. S.: Using satellite remote sensing to](#)
1095 [extrapolate evapotranspiration in time and space over a semiarid rangeland, Remote Sens.](#)
1096 [Environ., 49, 275-286, 1994.](#)

1097 [Liu, Y. Y., de Jeu, R. A. M., McCabe, M. F., Evans, J. P., and van Dijk, A. I. J. M.: Global long-term passive](#)
1098 [microwave satellite-based retrievals of vegetation optical depth, Geophys. Res. Lett., 38, L18402,](#)
1099 [2011a.](#)

1100 [Liu, Y. Y., Dorigo, W. A., Parinussa, R. M., De Jeu, R. A. M., Wagner, W., McCabe, M. F., Evans, J. P., and](#)
1101 [Van Dijk, A. I. J. M.: Trend-preserving blending of passive and active microwave soil moisture](#)
1102 [retrievals, Remote Sensing of Environment, 123, 280-297, 2012.](#)

1103 [Liu, Y. Y., Parinussa, R. M., Dorigo, W. A., De Jeu, R. A. M., Wagner, W., M. Van Dijk, A. I. J., McCabe, M.](#)
1104 [F., and Evans, J. P.: Developing an improved soil moisture dataset by blending passive and active](#)
1105 [microwave satellite-based retrievals, Hydrol. Earth Syst. Sci., 15, 425-436, 2011b.](#)

1106 [Liu, Y. Y., van Dijk, A. I. J. M., McCabe, M. F., Evans, J. P., and de Jeu, R. A. M.: Global vegetation biomass](#)
1107 [change \(1988-2008\) and attribution to environmental and human drivers, Global Ecology and](#)
1108 [Biogeography, 22, 692-705, 2013.](#)

1109 [Lokupitiya, E., Denning, S., Paustian, K., Baker, I., Schaefer, K., VERMA, S., MEYERS, T., Bernacchi, C. J.,](#)
1110 [SUYKER, A., and Fischer, M.: Incorporation of crop phenology in Simple Biosphere Model \(SiBcrop\)](#)

1111 [to improve land-atmosphere carbon exchanges from croplands, Biogeosciences, 6, 1103 - 1103,](#)
1112 [2009.](#)

1113 [Luoju, K., Pulliainen, J., Takala, M., Lemmetyinen, J., Derksen, C., and Wang, L.: Snow water equivalent](#)
1114 [\(SWE\) product guide, Global Snow Monitoring for Climate Research, 1, 2010.](#)

1115

1116 [Mach, D. M., Christian, H. J., Blakeslee, R. J., Boccippio, D. J., Goodman, S. J., and Boeck, W. L.:](#)
1117 [Performance assessment of the optical transient detector and lightning imaging sensor, Journal of](#)
1118 [Geophysical Research: Atmospheres \(1984–2012\), 112, 2007.](#)

1119 [McCabe, M. F. and Wood, E. F.: Scale influences on the remote estimation of evapotranspiration using](#)
1120 [multiple satellite sensors, Remote Sensing of Environment, 105, 271-285, 2006.](#)

1121 [McCabe, M. F., Wood, E. F., Wójcik, R., Pan, M., Sheffield, J., Gao, H., and Su, H.: Hydrological](#)
1122 [consistency using multi-sensor remote sensing data for water and energy cycle studies, Remote](#)
1123 [Sensing of Environment, 112, 430-444, 2008.](#)

1124 [Merlin, O., Al Bitar, A., Rivalland, V., Béziat, P., Ceschia, E., and Dedieu, G.: An analytical model of](#)
1125 [evaporation efficiency for unsaturated soil surfaces with an arbitrary thickness, Journal of Applied](#)
1126 [Meteorology and Climatology, 50, 457-471, 2011.](#)

1127 [Michel, D., Jiménez C., Miralles D. G., Jung M., Hirschi M., Ershadi A., Martens B., McCabe M. F., Fisher J.](#)
1128 [B., Mu Q., Seneviratne S. I., Wood E. F. and Fernández-Prieto D.: The WACMOS-ET project – Part](#)
1129 [1: Tower-scale evaluation of four remote sensing-based evapotranspiration algorithms, Hydrol.](#)
1130 [Earth Syst. Sci. Discuss., 12\(10\): 10739-10787, 2015](#)

1131 [Miralles, D. G., De Jeu, R. A. M., Gash, J. H., Holmes, T. R. H., and Dolman, A. J.: Magnitude and variability](#)
1132 [of land evaporation and its components at the global scale, Hydrol. Earth Syst. Sci., 15, 967-981,](#)
1133 [2011a.](#)

1134 [Miralles, D. G., Gash, J. H., Holmes, T. R. H., de Jeu, R. A. M., and Dolman, A.: Global canopy interception](#)
1135 [from satellite observations, Journal of Geophysical Research, 115, D16122, 2010.](#)

1136 [Miralles, D. G., Holmes, T. R. H., De Jeu, R. A. M., Gash, J. H., Meesters, A. G. C. A., and Dolman, A. J.:](#)
1137 [Global land-surface evaporation estimated from satellite-based observations, Hydrol. Earth Syst.](#)
1138 [Sci., 15, 453-469, 2011b.](#)

1139 [Miralles, D. G., Teuling, A. J., van Heerwaarden, C. C., and de Arellano, J. V.-G.: Mega-heatwave](#)
1140 [temperatures due to combined soil desiccation and atmospheric heat accumulation, Nature](#)
1141 [Geoscience, 7, 345-349, 2014a.](#)

1142 [Miralles, D. G., van den Berg, M. J., Gash, J. H., Parinussa, R. M., de Jeu, R. A. M., Beck, H. E., Holmes, T.](#)
1143 [R. H., Jiménez, C., Verhoest, N. E. C., and Dorigo, W. A.: El Niño–La Niña cycle and recent trends in](#)
1144 [continental evaporation, Nature Climate Change, 4, 122-126, 2014b.](#)

1145 [Miralles, D. G., Jiménez C., Jung M., Michel D., Ershadi A., McCabe M. F., Hirschi M., Martens B., Dolman](#)
1146 [A. J., Fisher J. B., Mu Q., Seneviratne S. I., Wood E. F. and Fernández-Prieto D.: The WACMOS-ET](#)
1147 [project – Part 2: Evaluation of global terrestrial evaporation data sets, Hydrol. Earth Syst. Sci.](#)
1148 [Discuss., 12\(10\): 10651-10700, 2015](#)

1149 [Monteith, J. L.: Evaporation and environment, Symp. Soc. Exp. Biol., 19, 205-234, 1965.](#)

1150 [Mu, Q., Heinsch, F. A., Zhao, M., and Running, S. W.: Development of a global evapotranspiration](#)
1151 [algorithm based on MODIS and global meteorology data, Remote Sensing of Environment, 111,](#)
1152 [519-536, 2007.](#)

1153 [Mu, Q., Zhao, M., Kimball, J. S., McDowell, N. G., and Running, S. W.: A Remotely Sensed Global](#)
1154 [Terrestrial Drought Severity Index, Bulletin of the American Meteorological Society, 94, 83-98,](#)
1155 [2012.](#)

1156 [Mu, Q., Zhao, M., and Running, S. W.: Improvements to a MODIS global terrestrial evapotranspiration](#)
1157 [algorithm, Remote Sensing of Environment, 115, 1781-1800, 2011.](#)

1158 [Mu, Q., Zhao, M., and Running, S. W.: MODIS Global Terrestrial Evapotranspiration \(ET\) Product \(NASA](#)
1159 [MOD16A2/A3\), Algorithm Theoretical Basis Document, Collection, 5, 2013.](#)

1160 [Mueller, B., Hirschi, M., Jimenez, C., Ciais, P., Dirmeyer, P. A., Dolman, A. J., Fisher, J. B., Jung, M.,](#)
1161 [Ludwig, F., Maignan, F., Miralles, D., McCabe, M. F., Reichstein, M., Sheffield, J., Wang, K. C.,](#)
1162 [Wood, E. F., Zhang, Y., and Seneviratne, S. I.: Benchmark products for land evapotranspiration:](#)
1163 [LandFlux-EVAL multi-dataset synthesis, Hydrol. Earth Syst. Sci. Discuss., 10, 769-805, 2013.](#)

1164 [Mueller, B., Seneviratne, S. I., Jimenez, C., Corti, T., Hirschi, M., Balsamo, G., Ciais, P., Dirmeyer, P.,](#)
1165 [Fisher, J. B., Guo, Z., Jung, M., Maignan, F., McCabe, M. F., Reichle, R., Reichstein, M., Rodell, M.,](#)
1166 [Sheffield, J., Teuling, A. J., Wang, K., Wood, E. F., and Zhang, Y.: Evaluation of global observations-](#)

1167 [based evapotranspiration datasets and IPCC AR4 simulations, Geophysical Research Letters, 38,](#)
1168 [2011.](#)

1169 [Nash, J. E. and Sutcliffe, J. V.: River flow forecasting through conceptual models: Part I - a discussion of](#)
1170 [principles, Journal of Hydrology, 10, 282-290, 1970.](#)

1171 [Nesbitt, S. W., Zipser, E. J., and Kummerow, C. D.: An examination of version-5 rainfall estimates from](#)
1172 [the TRMM Microwave Imager, precipitation radar, and rain gauges on global, regional, and storm](#)
1173 [scales, J. Appl. Meteorol., 43, 1016-1036, 2004.](#)

1174 [Norman, J. M., Kustas, W. P., and Humes, K. S.: Source approach for estimating soil and vegetation](#)
1175 [energy fluxes in observations of directional radiometric surface temperature, Agricultural and](#)
1176 [Forest Meteorology, 77, 263-293, 1995.](#)

1177

1178 [Otkin, J. A., Anderson, M. C., Hain, C., and Svoboda, M.: Examining the Relationship between Drought](#)
1179 [Development and Rapid Changes in the Evaporative Stress Index, Journal of Hydrometeorology,](#)
1180 [15, 938-956, 2014.](#)

1181 [Penman, H. L.: Natural Evaporation from Open Water, Bare Soil and Grass, Proceedings of the Royal](#)
1182 [Society of London. Series A. Mathematical and Physical Sciences, 193, 120-145, 1948.](#)

1183 [Potter, C. S., Randerson, J. T., Field, C. B., Matson, P. A., Vitousek, P. M., Mooney, H. A., and Klooster, S.](#)
1184 [A.: Terrestrial ecosystem production: a process model based on global satellite and surface data,](#)
1185 [Global Biogeochemical Cycles, 7, 811-841, 1993.](#)

1186 [Priestley, C. H. B. and Taylor, R. J.: On the Assessment of Surface Heat Flux and Evaporation Using Large-](#)
1187 [Scale Parameters, Mon. Weather Rev., 100, 81-92, 1972.](#)

1188 [Rebmann, C., Göckede, M., Foken, T., Aubinet, M., Aurela, M., Berbigier, P., Bernhofer, C., Buchmann,](#)
1189 [N., Carrara, A., and Cescatti, A.: Quality analysis applied on eddy covariance measurements at](#)
1190 [complex forest sites using footprint modelling, Theor Appl Climatol, 80, 121-141, 2005.](#)

1191 [Reichstein, M., Rey, A., Freibauer, A., Tenhunen, J., Valentini, R., Banza, J., Casals, P., Cheng, Y.,](#)
1192 [Grünzweig, J. M., and Irvine, J.: Modeling temporal and large - scale spatial variability of soil](#)
1193 [respiration from soil water availability, temperature and vegetation productivity indices, Global](#)
1194 [biogeochemical cycles, 17, 2003.](#)

1195 [Richardson, A. D., Black, T. A., Ciais, P., Delbart, N., Friedl, M. A., Gobron, N., Hollinger, D. Y., Kutsch, W.](#)
1196 [L., Longdoz, B., and Luyssaert, S.: Influence of spring and autumn phenological transitions on](#)
1197 [forest ecosystem productivity, Philosophical Transactions of the Royal Society B: Biological](#)
1198 [Sciences, 365, 3227-3246, 2010.](#)

1199 [Richey, A. S., Thomas, B. F., Lo, M.-H., Reager, J. T., Famiglietti, J. S., Voss, K., Swenson, S., and Rodell,](#)
1200 [M.: Quantifying renewable groundwater stress with GRACE, Water Resources Research, doi:](#)
1201 [10.1002/2015WR017349, 2015. n/a-n/a, 2015.](#)

1202 [Rubel, F. and Kottek M.: Observed and projected climate shifts 1901-2100 depicted by world maps of](#)
1203 [the Köppen-Geiger climate classification, Meteorologische Zeitschrift, 19\(2\): 135-141, 2010.](#)

1204 [Saha, S., Moorthi, S., Pan, H.-L., Wu, X., Wang, J., Nadiga, S., Tripp, P., Kistler, R., Woollen, J., and](#)
1205 [Behringer, D.: The NCEP climate forecast system reanalysis, Bulletin of the American](#)
1206 [Meteorological Society, 91, 1015-1057, 2010.](#)

1207 [Sahoo, A. K., Pan, M., Troy, T. J., Vinukollu, R. K., Sheffield, J., and Wood, E. F.: Reconciling the global](#)
1208 [terrestrial water budget using satellite remote sensing, Remote Sensing of Environment, 115,](#)
1209 [1850-1865, 2011.](#)

1210 [Saigusa, N., Ichii, K., Murakami, H., Hirata, R., Asanuma, J., Den, H., Han, S. J., Ide, R., Li, S. G., and Ohta,](#)
1211 [T.: Impact of meteorological anomalies in the 2003 summer on Gross Primary Productivity in East](#)
1212 [Asia, Biogeosciences, 7, 641-655, 2010.](#)

1213 [Scott, R. L.: Using watershed water balance to evaluate the accuracy of eddy covariance evaporation](#)
1214 [measurements for three semiarid ecosystems, Agricultural and Forest Meteorology, 150, 219-225,](#)
1215 [2010.](#)

1216 [Sheffield, J., Ferguson, C. R., Troy, T. J., Wood, E. F., and McCabe, M. F.: Closing the terrestrial water](#)
1217 [budget from satellite remote sensing, Geophysical Research Letters, 36, n/a-n/a, 2009.](#)

1218 [Sheffield, J., Wood, E. F., and Munoz-Arriola, F.: Long-term regional estimates of evapotranspiration for](#)
1219 [Mexico based on downscaled ISCCP data, Journal of Hydrometeorology, 11, 253-275, 2010.](#)

1220 [Shuttleworth, W. J. and Wallace, J. S.: Evaporation from sparse crops-an energy combination theory, Q.](#)
1221 [J. R. Meteorol. Soc., 111, 839-855, 1985.](#)

1222 [Simard, M., Pinto, N., Fisher, J. B., and Baccini, A.: Mapping forest canopy height globally with](#)
1223 [spaceborne lidar, Journal of Geophysical Research: Biogeosciences, 116, G04021, 2011.](#)

1224 [Smith, P., Lanigan, G., Kutsch, W. L., Buchmann, N., Eugster, W., Aubinet, M., Ceschia, E., Béziat, P.,](#)
1225 [Yeluripati, J. B., and Osborne, B.: Measurements necessary for assessing the net ecosystem carbon](#)
1226 [budget of croplands, Agriculture, ecosystems & environment, 139, 302-315, 2010.](#)

1227 [Sobrino, J. A., Jiménez-Muñoz, J. C., and Paolini, L.: Land surface temperature retrieval from LANDSAT](#)
1228 [TM 5, Remote Sensing of Environment, 90, 434-440, 2004.](#)

1229 [Soudani, K., Hmimina, G., Dufrêne, E., Berveiller, D., Delpierre, N., Ourcival, J.-M., Rambal, S., and Joffre,](#)
1230 [R.: Relationships between photochemical reflectance index and light-use efficiency in deciduous](#)
1231 [and evergreen broadleaf forests, Remote Sensing of Environment, 144, 73-84, 2014.](#)

1232 [Sprintsin, M., Cohen, S., Maseyk, K., Rotenberg, E., Grünzweig, J., Karnieli, A., Berliner, P., and Yakir, D.:](#)
1233 [Long term and seasonal courses of leaf area index in a semi-arid forest plantation, Agricultural and](#)
1234 [Forest Meteorology, 151, 565-574, 2011.](#)

1235 [Stackhouse, P. W., Gupta, S. K., Cox, S. J., Zhang, T., Mikovitz, J. C., and Hinkelman, L. M.: The](#)
1236 [NASA/GEWEX surface radiation budget release 3.0: 24.5-year dataset, GEWEX News, 21, 10-12,](#)
1237 [2011.](#)

1238 [Stoy, P. C., Mauder, M., Foken, T., Marcolla, B., Boegh, E., Ibrom, A., Arain, M. A., Arneth, A., Aurela, M.,](#)
1239 [and Bernhofer, C.: A data-driven analysis of energy balance closure across FLUXNET research sites:](#)
1240 [The role of landscape scale heterogeneity, Agricultural and forest meteorology, 171, 137-152,](#)
1241 [2013.](#)

1242 [Su, H., McCabe, M. F., Wood, E. F., Su, Z., and Prueger, J. H.: Modeling evapotranspiration during](#)
1243 [SMACEX: Comparing two approaches for local- and regional-scale prediction, Journal of](#)
1244 [Hydrometeorology, 6, 910-922, 2005.](#)

1245 [Su, Z.: The Surface Energy Balance System \(SEBS\) for estimation of turbulent heat fluxes, Hydrol. Earth](#)
1246 [Syst. Sci., 6, 85-100, 2002.](#)

1247 [Sulkava, M., Luyssaert, S., Zehle, S., and Papale, D.: Assessing and improving the representativeness of](#)
1248 [monitoring networks: The European flux tower network example, Journal of Geophysical](#)
1249 [Research, 116, 2011.](#)

1250 [Tucker, C. J., Pinzon, J. E., Brown, M. E., Slayback, D. A., Pak, E. W., Mahoney, R., Vermote, E. F., and El](#)
1251 [Saleous, N.: An extended AVHRR 8 - km NDVI dataset compatible with MODIS and SPOT](#)
1252 [vegetation NDVI data, Int. J. Remote Sens., 26, 4485-4498, 2005.](#)

1253 [van der Kwast, J., Timmermans, W., Gieske, A., Su, Z., Olivos, A., Jia, L., Elbers, J., Karssen, D., and de](#)
1254 [Jong, S.: Evaluation of the Surface Energy Balance System \(SEBS\) applied to ASTER imagery with](#)
1255 [flux-measurements at the SPARC 2004 site \(Barrax, Spain\), Hydrol. Earth Syst. Sci., 13, 1337-1347,](#)
1256 [2009.](#)

1257 [Veenendaal, M., Kolle, O., and Lloyd, J.: Seasonal variation in energy fluxes and carbon dioxide exchange](#)
1258 [for a broad leaved semi-arid savanna \(Mopane woodland\) in Southern Africa, Global Change](#)
1259 [Biology, 10, 318 - 328, 2004.](#)

1260 [Vinukollu, R. K., Sheffield, J., Wood, E. F., Bosilovich, M. G., and Mocko, D.: Multimodel Analysis of](#)
1261 [Energy and Water Fluxes: Intercomparisons between Operational Analyses, a Land Surface Model,](#)
1262 [and Remote Sensing, Journal of Hydrometeorology, 13, 3-26, 2011a.](#)

1263 [Vinukollu, R. K., Wood, E. F., Ferguson, C. R., and Fisher, J. B.: Global estimates of evapotranspiration for](#)
1264 [climate studies using multi-sensor remote sensing data: Evaluation of three process-based](#)
1265 [approaches, Remote Sensing of Environment, 115, 801-823, 2011b.](#)

1266 [Weligepolage, K., Gieske, A. S. M., van der Tol, C., Timmermans, J., and Su, Z.: Effect of sub-layer](#)
1267 [corrections on the roughness parameterization of a Douglas fir forest, Agricultural and Forest](#)
1268 [Meteorology, 162-163, 115-126, 2012.](#)

1269 [Wharton, S., Schroeder, M., Paw U, K. T., Falk, M., and Bible, K.: Turbulence considerations for](#)
1270 [comparing ecosystem exchange over old-growth and clear-cut stands for limited fetch and](#)
1271 [complex canopy flow conditions, Agricultural and Forest Meteorology, 149, 1477-1490, 2009.](#)

1272 [Wohl, E., Barros, A., Brunsell, N., Chappell, N. A., Coe, M., Giambelluca, T., Goldsmith, S., Harmon, R.,](#)
1273 [Hendrickx, J. M. H., Juvik, J., McDonnell, J., and Ogden, F.: The hydrology of the humid tropics,](#)
1274 [Nature Clim. Change, 2, 655-662, 2012.](#)

1275 [Yan, Y., Zhao, B., Chen, J., Guo, H., Gu, Y., Wu, Q., and Li, B.: Closing the carbon budget of estuarine](#)
1276 [wetlands with tower - based measurements and MODIS time series, Global Change Biology, 14,](#)
1277 [1690-1702, 2008.](#)

1278 [Yao, Y., Liang, S., Li, X., Hong, Y., Fisher, J. B., Zhang, N., Chen, J., Cheng, J., Zhao, S., and Zhang, X.:](#)
1279 [Bayesian multimodel estimation of global terrestrial latent heat flux from eddy covariance,](#)
1280 [meteorological, and satellite observations, Journal of Geophysical Research: Atmospheres, 119,](#)
1281 [4521-4545, 2014.](#)

1282 [Zhu, Z., Bi, J., Pan, Y., Ganguly, S., Anav, A., Xu, L., Samanta, A., Piao, S., Nemani, R. R., and Myneni, R. B.:](#)
1283 [Global data sets of vegetation leaf area index \(LAI\) 3g and Fraction of Photosynthetically Active](#)
1284 [Radiation \(FPAR\) 3g derived from Global Inventory Modeling and Mapping Studies \(GIMMS\)](#)
1285 [Normalized Difference Vegetation Index \(NDVI3g\) for the period 1981 to 2011, Remote Sensing, 5,](#)
1286 [927-948, 2013.](#)

1287 [Zierl, B., Bugmann, H., and Tague, C. L.: Water and carbon fluxes of European ecosystems: An evaluation](#)
1288 [of the ecohydrological model RHESSys, Hydrological processes, 21, 3328-3339, 2007.](#)

1289 ▼

Matthew McCabe 13/12/2015 3:48 PM

Deleted: Adler, R.F. et al., 2003. The version-2 global precipitation climatology project (GPCP) monthly precipitation analysis (1979-present). Journal of Hydrometeorology, 4(6): 1147-1167. ... [1]

1296 Table 1: Summary of data sources for tower-based and grid-based analysis and their spatial and
 1297 temporal resolutions.

Variable	Tower-based	Grid-based	Model
Air temperature	Tower data aggregated to 3-hourly	LandFlux data at 0.5° and 3-hourly	All models
Humidity	Tower-based relative humidity converted to specific humidity and aggregated to 3-hourly	Specific humidity from LandFlux data at 0.5° and 3-hourly	All except GLEAM
Pressure	Calculated as a function of ground elevation	LandFlux data at 0.5° and 3-hourly	All models
Net radiation	Tower data aggregated to 3-hourly	LandFlux data from SRB v3 at 1° and 3-hourly	All models
Ground heat flux	Tower data aggregated to 3-hourly	Calculated from net radiation and fractional vegetation cover data, 0.5° and 3-hourly	All models
Land surface temperature	Calculated from tower-based longwave upward radiation and aggregated to 3-hourly	LandFlux data at 0.5° and 3-hourly	SEBS only
Wind speed	Tower data aggregated to 3-hourly	LandFlux data at 0.5° and 3-hourly	SEBS only
Canopy height	Tower meta data	JPL product and Equation 1	SEBS only
NDVI	GIMMS NDVI at 8km and bi-monthly	GIMMS NDVI at 0.5° and bi-monthly	All except GLEAM
Leaf area index	Calculated from NDVI	LandFlux data at 0.5° and monthly	SEBS and PM-Mu
Fractional vegetation cover	Not used as ground heat flux is available.	Calculated from NDVI	All except GLEAM
Precipitation	Tower data aggregated to 3-hourly	LandFlux data at 0.5° and 3-hourly	GLEAM only
Soil properties	IGBP-DIS at 5 arc-minutes	IGBP-DIS data aggregated to 0.5°	GLEAM only
Soil moisture	CCI-WACMOS data at 0.25° and daily	Same as tower-based	GLEAM only
Soil depth	GlobSnow (daily and 25 km)	Same as tower-based	GLEAM only
Vegetation optical depth	From Liu et al. (2011b) at 0.25° and daily	Same as tower-based	GLEAM only
Snow water equivalent	GlobSnow and NSIDC at 0.25° and daily	Same as tower-based	GLEAM only
Lightning frequency	Monthly climatology at 0.5°	Same as tower-based	GLEAM only
Cover fractions	MOD44B data at 250 m	MOD44B data at 0.5°	GLEAM only

1299 Figure 1: Location of the selected towers and their distributions for various biomes

1300 Figure 2: Scatterplots of observed versus simulated latent heat flux for tower-based data.
1301 Colors show the frequency of values from high (red) to low (yellow). The thick black line
1302 represents the linear regression, while the thin line is the 1:1 line. The series of small circles
1303 show the percentile increments of data from the 1st to 99th, with large circles denoting the 25th,
1304 50th and 75th percentiles. The statistics shown on each figure provide coefficient of
1305 determination (R^2), slope (m), y-intercept (b), number of data records (n), the root-mean-
1306 squared difference (RMSD), relative error (RE) and the Nash-Sutcliffe Efficiency (NSE).

1307 Figure 3: Scatterplots of observed versus simulated evaporation for grid-based data. Colors
1308 show the frequency of values from high (red) to low (yellow). The thick black line is the linear
1309 regression and the thin line is the 1:1 line. The series of small circles show the percentile
1310 increments of data from the 1st to 99th, with large circles denoting the 25th, 50th and 75th
1311 percentiles. The statistics shown on the graphs are coefficient of determination (R^2), slope (m),
1312 y-intercept (b), number of data records (n), the root-mean-squared difference (RMSD), relative
1313 error (RE) and the Nash-Sutcliffe Efficiency (NSE).

1314 Figure 4: Comparison of the performance skill of the models in reproducing evaporation for the
1315 tower-based analyses. R^2 is the coefficient of determination, RE is relative error (lower is better)
1316 and NSE is the Nash-Sutcliffe Efficiency (higher is better). Towers are arranged from left to right
1317 based on aridity index.

1318 Figure 5: Coefficient of determination (R^2), relative error (RE) and Nash-Sutcliffe Efficiency (NSE)
1319 for models across different biome types. Each point represents the collection of all available 3-
1320 hourly records of towers located within the selected biome, with the number of towers shown
1321 on the secondary y-axis of the R^2 plot in red. NSE for the shrubland response of SEBS is printed.

1322

1323 Figure 6: Percentile plots of observed (x-axis) versus estimated latent heat flux (y-axis) at 3-
1324 hourly resolution for the tower-based analysis across the seven studied biomes. Percentiles
1325 encompass the 1st to 99th range in 1 percent increments, with Q_{25} , Q_{50} and Q_{75} denoted by large
1326 coloured circles.

1327 Figure 7: The upper panel presents Nash-Sutcliffe Efficiency (NSE; x-axis) and R^2 (color tone)
1328 between tower- and grid-based values for net radiation, land surface temperature, air
1329 temperature, wind speed, specific humidity, fractional vegetation cover and leaf area index,
1330 across the seven studied biome types. The lower panel presents the NSE (x-axis) and R^2 of
1331 model simulated evaporation against closure-corrected observed values. The number of towers
1332 for each biome type used in the analysis are shown in red font on the secondary (right) axis in
1333 each of the plots. Statistics for those results beyond the range of the x-axis are printed
1334 separately on the plot.

1335 Figure 8: Coefficient of determination (R^2), relative error (RE) and Nash-Sutcliffe Efficiency (NSE)
1336 for model simulated results across the five different climate zones (y-axis). The zones are
1337 represented by dryland (DRY), temperate continental (TempCONT), temperate (TEMP), sub-
1338 tropical (subTRO) and boreal (BOR). Each point represents the collection of all towers located
1339 within the selected climate zone, with the number of towers shown on the secondary y-axis of
1340 the R^2 panel in red.

1341 Figure 9: Percentile plots of observed (x-axis) versus estimated latent heat flux (y-axis) at 3-
1342 hourly resolution for tower-based analysis and across the different climate zones. Percentiles
1343 encompass the 1st to 99th range in 1 percent increments. Q_{25} , Q_{50} and Q_{75} are denoted by large
1344 circles.

1345

1346

1347 Figure 10: The upper panel shows Nash-Sutcliffe Efficiency (NSE; x-axis) and R^2 (color tone)
1348 between tower-based and grid-based values for net radiation, land surface temperature, air
1349 temperature, wind speed, specific humidity, fractional vegetation cover and leaf area index
1350 across the five different climate zones. The lower panel shows NSE (x-axis) and R^2 of model
1351 simulated evaporation against closure-corrected observed values across climate zones. The
1352 number of towers for each biome are shown in red font on the secondary (right) axis of the
1353 plots. Statistics for the grid-based SEBS result over dry climate zone are printed.

1354